



Universiteit
Leiden
The Netherlands

Deciphering fermionic matter: from holography to field theory

Meszéna, B.

Citation

Meszéna, B. (2016, December 21). *Deciphering fermionic matter: from holography to field theory*. *Casimir PhD Series*. Retrieved from <https://hdl.handle.net/1887/45226>

Version: Not Applicable (or Unknown)

License: [Licence agreement concerning inclusion of doctoral thesis in the Institutional Repository of the University of Leiden](#)

Downloaded from: <https://hdl.handle.net/1887/45226>

Note: To cite this publication please use the final published version (if applicable).

Cover Page



Universiteit Leiden



The handle <http://hdl.handle.net/1887/45226> holds various files of this Leiden University dissertation.

Author: Meszéna, B.

Title: Deciphering fermionic matter: from holography to field theory

Issue Date: 2016-12-21

Chapter 1

Introduction

One of the most challenging area in theoretical physics is that of strongly coupled many-body systems. Most of our knowledge and intuition come from perturbative descriptions especially in quantum mechanical systems. It is a priori rather remarkable that this seemingly limited tool can teach us so much about nature and can describe a large number of phenomena effectively. The modern understanding of this phenomenon is due to Wilson [1]. He introduced the idea of renormalization and universality which can be thought of as a metatheory of physical laws. Its strength relies on the fact that it is not necessary to refer closely to particular details of the system we wish to study. Wilsonian universality tells us that even given the unimaginably large number of possible interactions between the constituents, its consequences can be put into three categories with respect to its behavior at large distances. Most of the interactions turn out to be irrelevant and their effects are negligible at large distances. Only for a finite number of relevant couplings is the interaction important. In the marginal case, the interaction is equally important in the UV and in the IR. Therefore, universality tells us that many systems behave perturbatively at low energy, despite the fact that the couplings may be large at high energy.

There are also, however, systems (with relevant coupling), where we do know the microscopic physics but we do not have an algorithm which transforms a microscopic model to experimental predictions (which can be tested and compared to the model). This happens both in high-, and low-energy physics. The classical example is the theory of the strong force, QCD. It is perturbative at high energy (above $300MeV$), therefore it is possible to test the details of quark interaction in high-energy scattering experiment. However, QCD at everyday scales (describing for example the spectrum of mesons and baryons) is out of the range of applicability of weak-coupling physics. We will see in this thesis that many examples of such theories also exist in condensed matter physics. In these cases, one knows the UV theory very well (electrons interacting with each other

and with ions in the lattice via Coulomb interaction) but in some classes of materials we cannot predict macroscopic measurable properties such as conductivity or photoemission spectra in the IR regime (in which we are mostly interested).

This calls for new approaches. In bosonic systems it is possible to use Monte Carlo methods to calculate equilibrium quantities by considering the discretised version of the relevant quantum field theory in hand in imaginary time. The greatest achievements of this type of techniques is the determination of the proton mass with 2% accuracy using a discretised version of quantum chromodynamics [4]. It took, however, more than 20 years of research to achieve this goal and the power of a supercomputer due to the huge computational demands of the simulation (both in terms of CPU and memory). Even with their success, these numerical approaches have limited range of applicability.

Achieving this precision is only possible in equilibrium and it is even harder to simulate real time dynamics. For this, one would need to analytically continue the numerical data from imaginary to real time (from Matsubara frequencies to real frequencies) which would require the knowledge of the spectrum of very large frequencies with high accuracy. A common trick is to try to fit a physically motivated analytical expression (e.g. Pade approximant) to the high frequency regime.

A far more fundamental problem arises in fermionic strongly coupled system at finite density. These systems are especially hard to solve due to the fermion sign problem [2]. It means that even in an equilibrium Monte-Carlo simulation, the weight of each configuration is not a real, positive number as in the bosonic case but complex which leads to oscillatory behavior. It is in fact claimed that simulating fermionic systems is NP hard [2, 3].

Because of these difficulties of applying numerical methods to quantum many-body physics, investigating and improving analytical approaches is of high importance. In Chapter 2-4 of this thesis, we will apply several promising techniques to strongly correlated fermionic systems. To give a background, in this chapter, we will introduce these systems together with analytical, non-perturbative methods. Specifically, we will describe large- N methods, conformal field theories and holography (*AdS/CFT*).

1.1 Phases of fermionic matter: Fermi and non-Fermi liquids

1.1.1 Fermi liquids

Let us summarize first what are the most important characteristics of the most common fermionic system for which we do have a successful description: the Fermi liquid. Landau's Fermi liquid theory relies on the fact that the interactions become weak (they are irrelevant in the Wilsonian language) well below the scale of the Fermi momentum. This results in an infinitely long lived spectrum of quasiparticles at the Fermi surface. Though the values of explicit parameters (such as lifetime, quasiparticle residue) vary among materials, the qualitative features are the same.

Both theoretically and experimentally a very relevant quantity (which can be measured by ARPES) is the spectral function. This gives the spectrum of excitations and is computed through the imaginary part of the single particle Green's function. In case of a Fermi liquid with momentum near the Fermi surface, the form of the Green's function is:

$$G_R(k, \omega) = \frac{Z_k}{\omega - v_F(k - k_F) + \Sigma(k, \omega)} + G_{incoh}(k, \omega), \quad (1.1)$$

with the self energy being quadratic in the frequency and temperature [17] $\Sigma_{FL}(k, \omega) = iC_k(\omega^2 + T^2)$. At the Fermi surface ($\omega = 0$), the lifetime of the quasiparticle is infinite (at zero temperature), while for $\omega > 0$, it stays finite. The spectral function is given by

$$A(k, \omega) = \frac{ImG_R}{2\pi}, \quad (1.2)$$

and it is plotted in Fig. 1.1 for a free Fermi gas and an interacting Fermi liquid (at zero temperature). This quantity can be measured by inverse photoemission experiments (ARPES) and is a valuable tool to confirm either Fermi liquid behavior or deviation from it.

The occupation number (shown in Fig. 1.2) can be also calculated from the spectral function

$$n_k = \int_{-\infty}^0 d\omega A(k, \omega). \quad (1.3)$$

The quasiparticle residue Z_k sets the magnitude of the discontinuity at k_F in the occupation number.

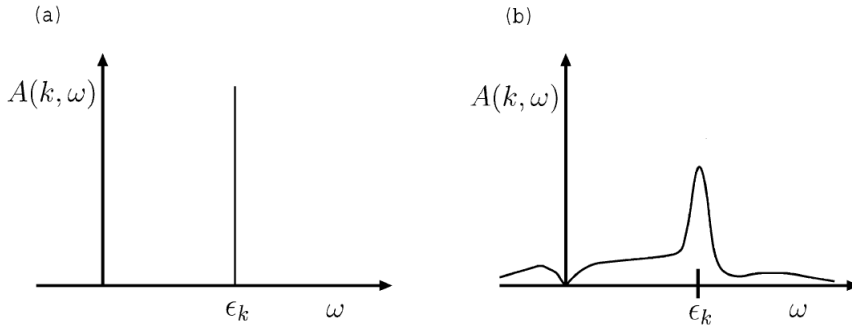


Figure 1.1. Spectral function as a function of frequency for a fixed momentum in the case of a a) free Fermi gas, b) interacting Fermi liquid (from [27]). The quasiparticle nature of these states is manifest in the form of a delta-function peak for the free Fermi gas. In case of the Fermi liquid, the peak broadens due to the interactions.

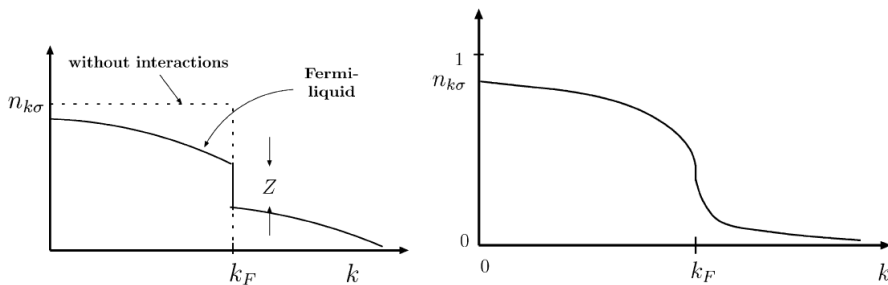


Figure 1.2. Occupation number of a a) Fermi liquid, b) marginal Fermi liquid, which we will introduce in Section 1.1.3 (from [27]).

1.1.2 Conductivity of Fermi liquids

Let us study another very relevant feature of a Fermi liquid: its resistivity. Experiments show that the DC resistivity scales as T^2 (as in Fig. 1.4) at low temperature (for a clean sample) when electron-electron scattering is the dominant process. The form of the spectral function we saw in the previous section and the temperature profile of the conductivity are not independent. Let us see how these two important experimental quantities are related to each other.

The frequency dependent conductivity is related to the retarded current-current correlator (Π^R) according to the Kubo formula

$$\sigma_{xx}(\omega) = -\lim_{\vec{q} \rightarrow 0} \left(\frac{1}{i\omega} \Pi_{xx}^R(\omega, \vec{q}) \right). \quad (1.4)$$

Here, the retarded quantity can be obtained from the Euclidean version using the usual analytical continuation

$$\Pi^R(\omega, \vec{q}) = \Pi(iq_n, \vec{q})|_{iq_n \rightarrow \omega + i\epsilon} \quad (1.5)$$

where in our notation $q = (iq_n, \vec{q})$ indicate both frequency and momentum dependence. As indicated we are interested in the diagonal part of the conductivity tensor.

The diagonal part of Π is defined by

$$\Pi_{xx}(q) = -T \langle J_x(q) J_x(-q) \rangle, \quad (1.6)$$

with $J_x(q)$ the momentum space current. Its form (depicted in Fig. 1.3) can be deduced from the $\psi^\dagger(x) \nabla \psi(x)$ real space expression:

$$J_x(q) \sim T \sum_{ik_n} \int d^d k (2k_x + q_x) \psi^\dagger(k) \psi(k+q), \quad (1.7)$$

where d is the number of space dimensions.

In general, in an interacting theory calculating (1.6) is difficult. Formally, there is an exact relation (Schwinger-Dyson equation) which connects it with the Green's function and three point vertex (Fig. 1.3):

$$\Pi_{xx}(iq_n, 0) = T \sum_{ik_n} \int d^d k (2k_x)^2 G\left(ik_n + iq_n, \vec{k}\right) G\left(ik_n, \vec{k}\right) \cdot \quad (1.8)$$

$$\cdot \Gamma\left(ik_n + iq_n, ik_n; \vec{k}, \vec{k}\right). \quad (1.9)$$

$$J_x(q) = \text{diagram} \quad \Pi_{xx}(q) = \text{diagram}$$

Figure 1.3. Left: Current vertex. Right: Schwinger-Dyson equation connecting the current-current correlator with the exact Green's function (double line) and irreducible three-point vertex (from [46]).

We can express the retarded version of Π by ignoring the vertex corrections (i.e. we set Γ to a constant) and using the substitution (1.5):

$$\Pi_{xx}^R(\omega, 0) = \int d^d k (2k_x)^2 \int_{-\infty}^{\infty} \frac{d\omega_1}{2\pi} \frac{d\omega_2}{2\pi} \frac{f(\omega_1) - f(\omega_2)}{\omega_1 - \omega - \omega_2 - i\epsilon} A(\omega_1, \vec{k}) A(\omega_2, \vec{k}), \quad (1.10)$$

where $f(\omega)$ is the Fermi-Dirac distribution. We have used the relation between the spectral function and the (Euclidean) Green's function

$$G(ik_n, \vec{k}) = \int_{-\infty}^{\infty} \frac{d\omega}{2\pi} \frac{A(\omega, \vec{k})}{ik_n - \omega}, \quad (1.11)$$

and the Matsubara sum

$$T \sum_{ik_n} \frac{1}{ik_n - \omega} = f(\omega). \quad (1.12)$$

We can obtain the DC conductivity from (1.10) by evaluating one of the frequency integral at infinitesimal ω

$$\sigma_{DC} \sim \int d^d k (2k_x)^2 d\omega_1 \frac{df(\omega_1)}{d\omega_1} \left(A(0, \vec{k}) \right)^2. \quad (1.13)$$

Ignoring the vertex correction is safe in case of the Fermi liquid (interaction is irrelevant). Note, however that this approximation is questionable for a system with relevant interactions.

One can simplify (1.13) by realizing that at low temperature, the derivative of the Fermi-Dirac distribution is a delta-function. Furthermore, the spectral function is highly peaked around the Fermi surface and in first approximation it only depends on k_{\perp} , the distance between \vec{k} and

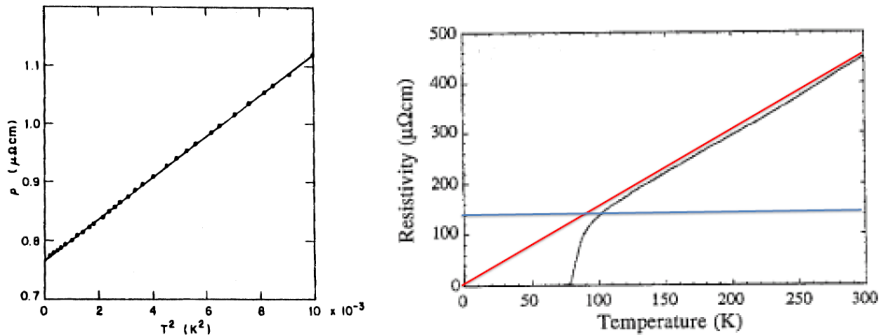


Figure 1.4. DC resistivity as a function of temperature in the case of a) Fermi liquid and b) non-Fermi liquid (from [28] and [29] respectively). The horizontal line represents the estimated Mott-Ioffe-Regel bound.

the Fermi surface. We can therefore approximate the conductivity as

$$\sigma_{DC} \sim k_F^{d+1} \int dk_{\perp} A(0, k_{\perp})^2. \quad (1.14)$$

Using that $\Sigma_{FL}(0, \vec{k}) = C \cdot iT^2$ for a Fermi liquid, we arrive at the formula

$$\sigma_{DC} \sim k_F^{d+1} \int dk_{\perp} \frac{\Sigma''^2}{((vk_{\perp})^2 + \Sigma''^2)^2} = k_F^{d+1} \int dk_{\perp} \frac{c \cdot T^4}{((vk_{\perp})^2 + c^2 T^4)^2}. \quad (1.15)$$

By changing the integration variable $k_{\perp} \rightarrow T^2 k_{\perp}$, we see that the temperature scaling of the conductivity is $\sigma_{DC} \sim T^2$. Strictly speaking, there is an oversight in this computation. In a translationally invariant system the DC conductivity is always infinite. A precise calculation that includes weak translational symmetry breaking (by introducing a lattice for example) gives the same answer, however.

1.1.3 Strongly correlated fermions: Non-Fermi liquids

In 1986, a remarkable discovery happened which was unexpected for most of the physics community: the discovery of high-temperature superconductivity in cuprate systems, where the resistivity dropped to zero at 34K [44, 43]. Soon, new compounds were found for which the critical temperature was above the boiling temperature of liquid nitrogen (77K). Until

then, the theory of superconductivity was believed to be completely described with the BCS theory: phonon interaction mediated Cooper pairs condense at low temperature. However, it predicts that the critical temperature can not be higher than $30K$. On further examination these new types of material turned out to display a lot more unconventional features other than its high critical temperature. A very notable surprising feature is that at temperature above T_c the normal (not superconducting) phase exhibits behavior which cannot be describe with Fermi liquid theory.

Many electronic materials have been discovered since which display unconventional behavior. What is common in these different systems is first of all the layered structure (with CuO_2 -planes in the case of the cuprates). This is believed to be the central cause of strongly coupled physics. This also means that important features of the system are captured by models in $d = 2$ spatial dimension. Secondly, these class of materials have a distinctive behavior as a function of a doping parameter x . These systems have very rich phase diagram. A simplified version of it is shown in Fig. 1.5. For large doping we have a normal Fermi liquid phase with sharp Fermi surface. In the other limit, for low doping the system is a Mott insulator with antiferromagnetic properties (or other type of phase). The most interesting regime is between these phases at intermediate doping. For low temperature, this is the exotic superconducting phase discovered in 1986.

The distinctive feature is that it is believed that under the superconducting dome there is a quantum critical point (QCP). The notion of a quantum critical point is very general and is important in bosonic systems as well. For a QCP to exist in a quantum system one needs a tunable parameter r in the Hamiltonian. This parameter can be for example an external magnetic field, pressure or the doping fraction as we described above in case of the cuprates. At zero temperature there can exist a critical value of this parameter r_c such that the groundstate of the system for $r < r_c$ can not be continuously deformed into the groundstate for $r > r_c$. In other word, the system undergo a zero temperature phase transition as one tune r . If this transition is second order at the critical point ($r = r_c$), all correlation function possess a scaling symmetry, i.e.

$$\vec{x} \rightarrow s\vec{x}, \quad t \rightarrow s^z t, \quad (1.16)$$

similarly to thermal phase transitions. The exponent z is called the dynamical critical exponent, and it tells us the different scaling between time

and spatial variables. If $\mathbf{z} = 1$, we are dealing with a relativistic system with scaling symmetry. In that case the symmetry group is conjectured to be always enhanced with the special conformal transformations, arriving at a conformal field theory (CFT). We will study CFTs in more depth in Section 1.2.2.

The quantum critical point although seems to be special just one point in the phase diagram. However, if we consider now the system at finite temperature, originated from the QCP the properties in a cone-like region are still governed by the QCP. In this region therefore, the physics is also universal. The cuprates (and also other types of strongly correlated materials) exhibit such a cone. This region is the strange metallic phase and it can be obtained by heating up the system near optimal doping (see in Fig. 1.5). This is in contrast with conventional superconductors described by BCS-theory, where the normal metallic phase is of a Landau Fermi liquid. This is why it is believed that high T_c superconductivity is governed by a QCP.

The strange metallic phase has linear- T resistivity (as opposed to the T^2 resistivity of Fermi liquids) up to very high temperatures (as is depicted in Fig. 1.4b). From this experimental fact (anomalously large resistivity in the normal phase) alone one can conclude that non-quasiparticle type of physics is at work. To see this, let us use the Drude formula to obtain a resistivity bound for quasiparticle transport. In that case, the resistivity can be expressed as a function of the scattering time τ

$$\rho = \frac{m}{ne^2\tau}, \quad (1.17)$$

where n is the density of charge carriers. For a quasiparticle, τ can be approximated by $v_F\tau \sim l_{MFP}$, where v_F is the Fermi velocity and l_{MFP} is the mean free path. The resistivity is therefore inversely proportional to the mean free path:

$$\rho \sim \frac{k_F}{ne^2} \cdot \frac{1}{l_{MFP}} < \frac{k_F}{ne^2} \cdot \frac{1}{a}. \quad (1.18)$$

However, the mean free path cannot be smaller than the lattice spacing of the material and therefore, an upper bound exists (the Mott-Ioffe-Regel bound) for the resistivity. If in a material, quasiparticle transport is at work, its resistivity should saturate at high temperature.

A phenomenological description of the strange metallic phase can be given in terms of the so-called marginal Fermi-liquid. In this approach

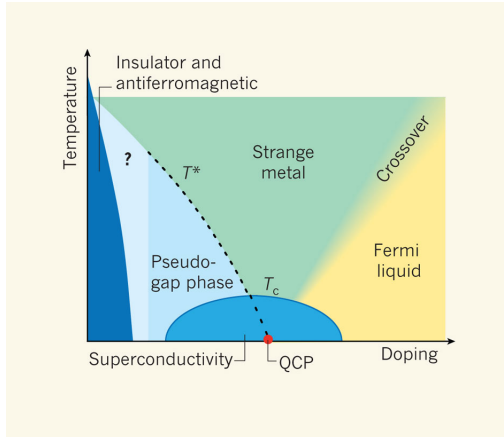


Figure 1.5. Schematic phase diagram of the cuprates (from [31]).

one fits the ARPES data (at low temperature) with the Green's function of the form [26]:

$$G_{MFL}(k, \omega) = \frac{Z}{v_F(k - k_F) - \omega - \Sigma(\omega)}, \quad (1.19)$$

with

$$\Sigma_{MFL}(\omega) = \lambda \left(\omega \log \left(\frac{x}{\omega_c} \right) - i \frac{\pi}{2} x \right), \quad (1.20)$$

where $x = \max(|\omega|, T)$. This results in an occupation number as in Fig. 1.2 b). Note that the discontinuity disappears, signaling again that we are not dealing with a gas of quasiparticles. Furthermore, as opposed to the Fermi liquid the self energy is completely independent of the momentum. We will see that this type of Green's function can be obtained by assuming that the fermions are interacting with a $\mathbf{z} = \infty$ critical system with large number of degrees of freedom. In this thesis we will meet other forms of Green's functions for non-Fermi liquids coming from different considerations.

We can connect this form of Green's function with the linear- T resistivity using (1.14) with $Im(\Sigma_{MFL}) \sim T$ and changing the integration variable to $k_{\perp} \rightarrow Tk_{\perp}$. We emphasise, however, that this derivation was based on the assumption that vertex-corrections can be neglected.

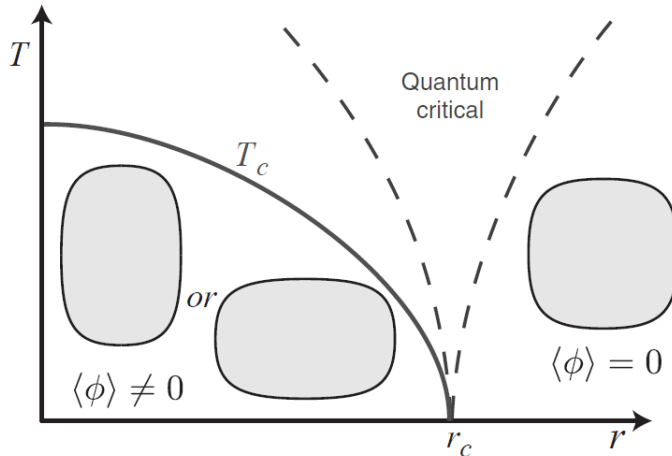


Figure 1.6. Phase diagram of the Ising-nematic transition (from [11]).

1.1.4 Ising-nematic transitions: quantum critical boson coupled to a Fermi surface

One can ask from a theoretical point of view, what kind of (effective) fermionic Lagrangian can result to non-Fermi liquid behavior. A natural attempt would be to introduce a four-fermion interaction between the fermions. However, in $d \geq 2$ such an interaction is generically irrelevant (with the well-known exception of BCS instability), therefore does not destroy the quasiparticle properties near the Fermi surface and we are still left with a Landau Fermi Liquid.

The simplest (continuum) model in which non-Fermi liquid behavior appears involves a fluctuating massless bosonic order parameter. The origin of the order parameter can be different, but for concreteness we will discuss the Ising-nematic transition observed for example in $YBa_2Cu_3O_y$ [30]. Here, in the unordered phase, the electronic correlations have C_4 rotation symmetry originated from the underlying lattice. In the ordered phase this rotation symmetry is spontaneously broken to C_2 as it is depicted in Fig. 1.6.

The order parameter can be described with the Landau-Ginzburg relativistic action [11]

$$S_b = \int d^d x d\tau \left[\frac{1}{2} \left((\partial_\tau \phi)^2 + (\nabla \phi)^2 + r \phi^2 \right) + u \phi^4 \right], \quad (1.21)$$

and the interaction with the fermions (we neglect the spin degrees of freedom of the fermions) is

$$S_{int} \sim \lambda \int d\tau \int d^d k d^d q d(k) \phi(q) \psi^+(k+q/2) \psi(k-q/2). \quad (1.22)$$

Of course, the free fermionic part of the action has the usual form of

$$S_f = \int d\tau \int \frac{d^d k}{(2\pi)^d} \psi^+(k) (\partial_\tau + \epsilon(k)) \psi(k). \quad (1.23)$$

In $d = 2$ dimensions, in which we are most interested, the coupling λ is relevant. The parameter which controls the quantum phase transition is the mass term r in the bosonic part. In the massive case $r > 0$ we can integrate out the boson below the scale $\omega < r$, therefore the shape of the Fermi surface does not change. For $r < 0$ however ϕ acquire a non-zero (uniform) expectation value $\langle \phi \rangle \neq 0$ and its effect on the fermions is such that the shape of the Fermi surface changes. To achieve the C_2 symmetric shape (as in Fig. 1.6) we can choose $d(k) \sim \cos k_x - \cos k_y$. The most interesting question however, is what happens to the system when we tune r to criticality ($r = 0$).

Hertz-Millis approach

The model in the previous section was studied already in the 70's by Hertz [15]. His approach was to integrate out the fermions and derive an effective action for the order parameter. After the evaluation of the fermionic path integral one obtains for the partition function

$$Z = \int \mathcal{D}\phi \det(G^{-1}[\phi]) e^{-S_b[\phi]} = \int \mathcal{D}\phi \exp(-S_b[\phi] - S_{det}[\phi]), \quad (1.24)$$

where $G^{-1}[\phi] \sim G_0^{-1} + \lambda\phi$, with G_0 being the free fermion propagator, is the inverse of the fermion Green's function in the presence of a scalar field in real space - we assume $d(k) = 1$ for simplicity. The effective action from the determinant can be formally written as

$$S_{det} = -Tr \log G^{-1}[\phi]. \quad (1.25)$$

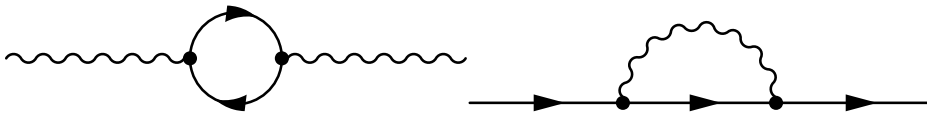


Figure 1.7. One-loop diagrams in the theory of fermions and quantum critical bosons. On the left: boson polarization diagram (Landau damping). On the right: fermion self energy correction.

This quantity has the usual non-local expansion in the coupling constant:

$$\text{Tr} \log G^{-1}[\phi] \sim \lambda^2 \int d^{d+1}X d^{d+1}Y G_0(X-Y)^2 \phi(X) \phi(Y) \quad (1.26)$$

$$+ \lambda^3 \int d^{d+1}X d^{d+1}Y d^{d+1}Z G_0(X-Y) G_0(Y-Z) \cdot \quad (1.27)$$

$$\cdot G_0(Z-X) \phi(X) \phi(Y) \phi(Z) + \dots, \quad (1.28)$$

involving closed fermion loops with n propagators which result in effective interaction terms in the form of ϕ^n . Here, we used the simplified notation X , Y and Z for the spatial coordinates and imaginary time variables. The assumption of the Hertz-Milis approach is that the terms with $n > 2$ can be neglected in the low frequency limit [15]. Therefore only the one-loop Landau damping diagram (see the left figure in Fig. 1.7) contributes to the boson correction. This has the form $\Pi_{LD} = \gamma \left| \frac{\omega}{k} \right|$ in momentum space [11].

We arrive therefore to the modified boson action after including the one-loop polarization

$$S_{\text{Hertz}} = \frac{1}{2} \int \frac{d^d k d\omega}{(2\pi)^{d+1}} \left(k^2 + \gamma \left| \frac{\omega}{k} \right| + r \right) |\phi(k, \omega)|^2 + u \int d^d x d\tau \phi^4(x, \tau).$$

The ω^2 bare kinetic term was neglected based on that for small frequencies the polarization (Landau damping) term dominates.

The quadratic part of this action is invariant under the scaling

$$\vec{x} \rightarrow s\vec{x}, \quad t \rightarrow s^z t, \quad \phi \rightarrow \phi s^{1-\frac{d+z}{2}} \quad (1.29)$$

if we choose \mathbf{z} to be 3. Using this we can deduce that the dimension of the quartic coupling u is $\dim[u] = 1 - d$. Therefore, under this scaling the boson self-interaction is irrelevant for $d > 1$.

However, the above argument of Hertz and Millis is questionable in the case of $d = 2$ dimensions. It ignores how the boson-fermion coupling λ scales, and in $d = 2$ it is relevant. In this case ignoring the terms with $n > 2$ from (1.28) is no longer self-consistently justified. Therefore, more careful analysis are needed for the problem. After the next section about large- N methods we will list some newer approaches from the literature. Then in Chapter 3 and 4 we will study the problem in detail in the so-called quenched approximation.

1.2 Non-perturbative methods

$d = 2$ fermions coupled to a QCP is an example of an important physical systems where perturbative methods cannot be applied. Therefore we need to seek alternative ways to deal with such problems. Non-perturbative methods are only exact in case of very special theories. For a reasonably generic case, one needs to use some form of approximation. Therefore, it is important to be familiar with more than one technique and to study the strongly coupled system at hand with several different approaches, since they can shed light to different aspects of the physics.

In this chapter we will give a brief introduction of some of these methods, namely large- N theories, conformal field theory and finally *AdS/CFT* correspondence (and holography in general). It is far from the complete list of important techniques, however. We must for example mention Wilsonian-, and functional renormalization group approaches, Monte-Carlo simulations and the use of dualities as the most successful ones. Integrability, supersymmetry and localization are also very useful and well studied methods with more limited applicability however than RG techniques.

1.2.1 Large- N theories

When dealing with strongly coupled systems one can not rely on the smallness of the coupling constant. Therefore, to gain insight of the system, it is possible to extend the theory with another parameter and use it as a control parameter. One standard way is to take multiple copies of the fields. This means adding additional degrees of freedom, therefore making the theory more classical than the original one. Large- N extensions have an important role in strongly coupled physics (both in condensed matter,

and high energy physics) on its own and they are crucial ingredients of the AdS/CFT correspondence as well.

Of course this extension can be implemented in different ways. We will review here the vector large- N and the matrix large- N models.

Vector large- N models

For the sake of concreteness, let us consider the following $O(N)$ bosonic model:

$$S = \int d^d x dt \left[-\frac{1}{2} \partial_\mu \phi_i \partial^\mu \phi^i - \frac{m^2}{2} \phi_i \phi^i - \frac{\lambda}{4!} (\phi_i \phi^i)^2 \right], \quad (1.30)$$

where $i = 1, \dots, N$ indicates the different species of bosons. This is called a vector model because ϕ transforms in the fundamental representation of $O(N)$. The coupling has the (naive) scaling dimension $3 - d$ therefore it is relevant in $d = 2$.

We can introduce a non-dynamical auxiliary field σ by writing

$$Z = \int D\phi \exp(-S) = c \cdot \int D\phi D\sigma \exp(-S_{\psi\sigma}), \quad (1.31)$$

where c is a field-independent, irrelevant constant. The extended action has the form

$$S_{\psi\sigma} = \int d^d x dt \left[-\frac{1}{2} \partial_\mu \phi_i \partial^\mu \phi^i - \frac{m^2}{2} \phi_i \phi^i + \frac{6}{\lambda} \sigma^2 - \sigma \phi_i \phi^i \right] \quad (1.32)$$

Since in this form the ϕ integrals are gaussian, we can evaluate the path integral explicitly

$$Z = c \cdot \int D\sigma \exp(-S_\sigma), \quad (1.33)$$

with

$$S_\sigma = N \int d^d x dt \left(\frac{6}{\lambda} \sigma^2 + \frac{i}{2} \log(-\square + m^2 + \sigma) \right), \quad (1.34)$$

where we have rescaled the coupling constant $\tilde{\lambda} = N\lambda$.

If N is large, then the path integral is dominated by the saddle point of S_σ and therefore, the theory can be analysed by semi-classical methods. Note, that we would arrive to similar results if we had started with N species of fermions transforming in the fundamental representation of $O(N)$. We have seen therefore that introducing N can help solving the original model.

Matrix large- N models

There is another way how one can introduce multiple similar degrees of freedom: by considering matrix valued fields. This is very natural in high-energy physics. The prime examples of the matrix valued large- N limit is the study of QCD and non-Abelian gauge theories in general. There the meaning of the parameter N there is the number of colors of the quarks (N_c). The theory has a local $SU(N_c)$ symmetry. The matter fields (quarks) transform in the fundamental representation, while the force-carriers (gluons) transforms in the adjoint matrix representation. The ($SU(N)$ invariant) action for the gauge-fields and quarks is

$$S = \int d^d x dt \left[-\frac{1}{4g_{YM}^2} \text{Tr} (F_{\mu\nu} F^{\mu\nu} + \bar{\psi} \gamma^\mu D_\mu \psi) \right], \quad (1.35)$$

where $D_\mu = \partial_\mu - iqA_\mu$ and the non-abelian field strength can be deduced from the matrix valued gauge connection

$$F_{\mu\nu} = \partial_\mu A_\nu - \partial_\nu A_\mu - i [A_\mu, A_\nu]. \quad (1.36)$$

The matrix form of the vector potential can be written as $A_\mu = A_\mu^a T_a$ with T_a being the generators of $SU(N)$.

However, the notion of matrix large- N limit is more general and can be applied to scalar field theories as well. Let's consider therefore the “ ϕ^4 type theory”:

$$S = \frac{1}{g^2} \int d^d x dt \left[\text{Tr} \left(-\partial_\mu \Phi^+ \partial^\mu \Phi - m^2 \Phi^+ \Phi \right) - \frac{1}{4!} \text{Tr} (\Phi^+ \Phi \Phi^+ \Phi) \right]. \quad (1.37)$$

The dynamics of this theory is different from the vector large- N case. First of all, note that the single trace structure of the interaction $\text{Tr} (\Phi^+ \Phi \Phi^+ \Phi)$ prevent us to introduce an auxiliary field in the form of (1.32). If we had a double trace type of interaction ($\text{Tr} (\Phi^+ \Phi) \text{Tr} (\Phi^+ \Phi)$) which is a different way of generalizing, the method of the previous section would apply. However, as we will see there is a notion of classicalisation here as well. For simplicity we will consider the symmetry group to be $U(N)$. As for gauge theories, Φ transforms in the adjoint representation $\Phi \rightarrow U^{-1} \Phi U$.

The interesting limit here was first introduced by t'Hooft [12]. He studied the special limit where one keeps the combination $\lambda = g^2 N$ fixed while taking $N \rightarrow \infty$. To determine the N dependence of Feynman diagrams it is very useful to introduce the so-called double line notation where for the

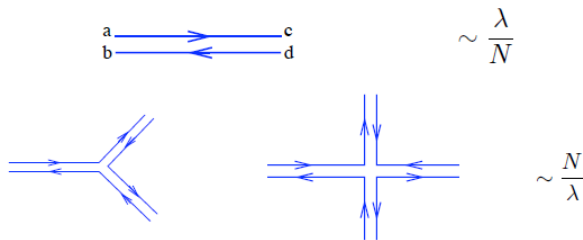


Figure 1.8. The propagator and vertices in a matrix theory with double line notation. The propagator scales as $1/N$, while each vertices as N^1 (from [45]).

propagators we draw two lines representing the two indices of the field Φ_j^i (see in Fig. 1.8). In this convention we can directly read off from (1.37) what is the N dependence of a diagram. A propagator contributes with $g^2 \sim \lambda/N$, while a vertex is proportional to N/λ . Furthermore, every index loop comes with an additional factor of N . We see therefore that the N dependence of a diagram is N^{V-P+L} , where V , P and L stand for the number of vertices, propagators and index loops respectively.

Note, that we can attach a topological meaning to this result. To demonstrate this, we consider vacuum diagrams. Let associate to each diagram a triangulation of a two dimensional manifold (as in Fig. 1.9) where the propagators are the edges, and the interior of each index loops are the faces. In this construction the exponent of the N dependence is $F - E + V = \chi = 2 - 2h$ (F , E and V are being the faces, edges and vertices of the triangulation respectively), which is the Euler characteristic of the triangulation with h the number of holes. $\chi = 2$ ($h = 0$) corresponds to a triangulation of a sphere, where $h \neq 0$ corresponds to a triangulation of a torus with h holes. Therefore, the more complex the topology of a diagram, the more subleading it is in terms of N .

The interesting quantities are correlation functions of $U(N)$ invariant (“gauge-invariant”) operators. If the symmetry is gauged then the physical observables are only single- and multitrace combination of the elementary fields: i.e. $Tr((\Phi^+\Phi)^n)$, $Tr(\Phi^+\Phi)Tr(\Phi^+\Phi)$. If the symmetry is not gauged then the physical Hilbert space is larger but we will still call these operators gauge-invariant and the consequences of the large- N limit will be identical.

Let’s first examine the two-point function of a single trace operator (we take $\mathcal{O}_4 = Tr(\Phi^+\Phi\Phi^+\Phi)$ for concreteness). We can write it as a

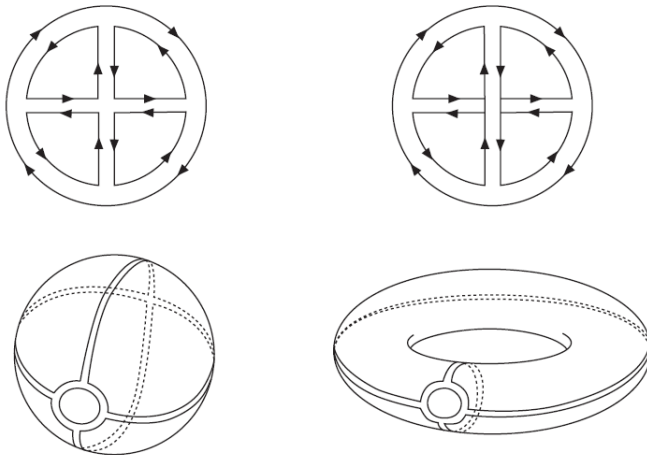


Figure 1.9. Two vacuum diagram in a matrix theory (with both cubic and quartic coupling). The left diagrams scales as N^2 , while the right as N^0 . This fact is also manifested in the fact that with the left diagram it is possible to triangulate a sphere while the right one only can be drawn to a torus (from [45]).

sum of the disconnected and connected component.

$$\langle \mathcal{O}_4 \mathcal{O}_4 \rangle = \langle \mathcal{O}_4 \rangle \langle \mathcal{O}_4 \rangle + \langle \mathcal{O}_4 \mathcal{O}_4 \rangle_c \quad (1.38)$$

Using the double line notation it is easy to see that while both the connected and the disconnected piece have the same number of vertices and propagators (at leading order), the connected one has less index loops (see in Fig. 1.10). Therefore if $\langle \mathcal{O}_4 \rangle$ is non-vanishing, the two-point function is dominated by the disconnected component. However, this expectation value is often zero (in a CFT it is always vanishing) and the leading behavior of the correlation function is non-trivial. The connected component scales as $\langle \mathcal{O}_4 \mathcal{O}_4 \rangle_c \sim N^2$ and therefore it become infinite in the $N \rightarrow \infty$ limit. To avoid this, one usually renormalizes the single-trace operators of the theory such that its connected two-point function does not scale with N (for example $\frac{1}{N} \mathcal{O}_4 = \tilde{\mathcal{O}}_4$). After this normalization there is no additional freedom in the definition of multi-trace operators.

In similar way we can show that the higher-point functions always factorizes. To illustrate this, let us consider the four point function of (the already properly normalized operator) $\mathcal{O}_2 = \frac{1}{N} \text{Tr}(\Phi^+ \Phi)$:

$$\langle \mathcal{O}_2 \mathcal{O}_2 \mathcal{O}_2 \mathcal{O}_2 \rangle = \langle \mathcal{O}_2 \mathcal{O}_2 \mathcal{O}_2 \mathcal{O}_2 \rangle_c + \langle \mathcal{O}_2 \mathcal{O}_2 \rangle_c \langle \mathcal{O}_2 \mathcal{O}_2 \rangle_c + \dots \quad (1.39)$$

$$\langle \mathcal{O}_4 \mathcal{O}_4 \rangle = \text{[Diagram 1]} + \text{[Diagram 2]} + \text{[Diagram 3]}$$

Figure 1.10. The two-point function of a single-trace operator can be split into a disconnected and a connected piece (from [8]). Both type of diagrams have the same number of propagators and vertices but the connected diagrams have less index loops, therefore they are subleading in N .

The disconnected piece (which can no longer vanish under any circumstances) scales as N^0 but the connected one goes to zero in the large- N limit.

$$\langle \mathcal{O}_2 \mathcal{O}_2 \mathcal{O}_2 \mathcal{O}_2 \rangle_c \sim N^{-2} \rightarrow 0. \quad (1.40)$$

As we will see in the forthcoming sections, the vanishing of the non-trivial component of higher point functions of single-trace operators in the large- N limit has important consequences in *AdS/CFT* as well.

Large- N approaches to quantum critical fermions

Large- N type approaches are important in condensed matter physics as well. As we have seen the quantum critical fermion model introduced in Section 1.1.4 in $d = 2$ dimensions is strongly coupled. To analyse the system (at least qualitatively) a usual approach is to generalize the theory and introduce multiple species of bosons (N_b) and fermions (N_f). One then can hope for a non-perturbative solution in a certain limit (typically large- N limit).

Since we have two parameters (N_b, N_f), there are in principle a lot of possible extension of the theory.

- One approach is to take the vector large- N_f limit while keeping $\lambda\sqrt{N_f}$ fixed [20, 21, 24]. In this case at one-loop the Landau damping (left of Fig. 1.7) or boson polarization diagram is $\mathcal{O}(N_f^0)$ but the fermion self energy correction (right of Fig. 1.7) is $\mathcal{O}(N_f^{-1})$. This limit is extensively studied by renormalization group methods up to four loops. However as pointed out in [24] it is questionable

whether it is a controllable expansion is since there are infinitely many diagrams with the same power of N_f .

- It is also possible to consider large N matrix theories with $SU(N)$ symmetry [26–29]. In this case the fermions transform in the fundamental representation (therefore there are $N_f = N$ number of them), while the bosons transform in the adjoint representation (so there are $N_b = N^2$ of them). The scaling of the coupling is chosen to be such that $\lambda\sqrt{N}$ is fixed similarly to the previous case (and the t’Hooft limit). Since $N_b \gg N_f$ the Landau damping is subleading compare to the fermion self energy. In the original problem ($N_f = N_b = 1$), the Landau damping believed to be an important effect at low frequencies. With this limit therefore one can qualitatively study the physics above this scale. At higher order for $N_f \rightarrow \infty$ the so-called rainbow diagrams give the dominant contributions to the self energy as we will explain in Chapter 3.

1.2.2 Conformal field theories

We now turn our attention to conformal field theories which are another type of important non-perturbative systems where we have (somewhat better) mathematical control. We have seen that studying critical points are crucial in understanding strongly correlated systems. In the Wilsonian language, at a general point in the RG flow one can compute the β function of the coupling (for example with momentum decimation)

$$\beta(g) = \mu \frac{\partial g}{\partial \mu} \quad (1.41)$$

When this function vanishes $\beta(g^*) = 0$ for some values (g^*) of the coupling, the renormalization group flow ends in fixed point and the system has the scaling symmetries (1.16). If the dynamical critical exponent is unity, i.e. time and spatial dimensions scales at the same way (the system is “relativistic”), these symmetries enhanced with the so-called special conformal symmetry and the system is conformally invariant. In most of the condensed matter applications, the vanishing β function is at only a special value of the coupling (g^*) so the critical point is isolated. We will see however, that in certain supersymmetric theories it is possible, that the β function vanishes for all values of the coupling.

This large symmetry group offers us another way to study strongly correlated systems non-perturbatively. 1 + 1 dimensional theories turned

out to be special in such a way that the symmetry group is even larger than in $d > 1$ spatial dimensions. In some cases (in the so-called minimal models and Liouville theory), this imposes such large constraints on the correlation functions that the theory can be solved exactly via the conformal bootstrap. This program was an active area of research in the 70's and 80's and recently it has received renewed attention with systems in higher dimensions. We will focus here on $d > 1$, and study features which are generic so we do not need to restrict ourselves to $1 + 1$ dimension.

Since the strategy with these systems is to squeeze out as much physics as possible from the symmetry properties we should start with the algebra. Let us study therefore the properties of this symmetry group (in $d > 1$) which is realized in $\mathbf{z} = 1$ critical points. For concreteness we will focus here on the Euclidean case. In the following table we summarize the (finite) coordinate transformations and its generators:

Transformation	Generator
Translation $x'^{\mu} = x^{\mu} + a^{\mu}$	$P_{\mu} = -i\partial_{\mu}$
Rotation $x'^{\mu} = M_{\nu}^{\mu}x^{\nu}$	$L_{\mu\nu} = i(x_{\mu}\partial_{\nu} - x_{\nu}\partial_{\mu})$
Dilatation $x'^{\mu} = sx^{\mu}$	$D = -ix^{\mu}\partial_{\mu}$
Special Conformal Transformation $x'^{\mu} = \frac{x^{\mu} - b^{\mu}x^2}{1 - 2b \cdot x + b^2x^2}$	$K_{\mu} = -i(2x_{\mu}x^{\nu}\partial_{\nu} - x^2\partial_{\mu})$

These generators satisfy the following algebra

$$[D, P_{\mu}] = iP_{\mu} \tag{1.42}$$

$$[D, K_{\mu}] = -iK_{\mu} \tag{1.43}$$

$$[K_{\mu}, P_{\nu}] = 2i(\eta_{\mu\nu}D - L_{\mu\nu}) \tag{1.44}$$

$$[K_{\rho}, L_{\mu\nu}] = i(\eta_{\rho\mu}K_{\nu} - \eta_{\rho\nu}K_{\mu}) \tag{1.45}$$

$$[P_{\rho}, L_{\mu\nu}] = i(\eta_{\rho\mu}P_{\nu} - \eta_{\rho\nu}P_{\mu}). \tag{1.46}$$

Here $\eta_{\mu\nu} = \text{diag}(1, \dots, 1)$ is the Euclidean metric.

This group is called the conformal group and denoted by $SO(d + 2, 1)$. It turns out that it is isomorphic to the group of Lorentz transformations in $d + 3$ dimensions. Note the somewhat unconventional notation for the number of dimensions. Although we are in Euclidean signature, we still denote the number of spacetime dimensions $d + 1$ (d spatial dimensions and an imaginary time dimension) to keep our notation consistent with

the previous sections. In other words the conformal group in certain dimensions is always isometric to the Lorentz algebra with two extra dimensions (one space-like and one time-like). In the same manner, if our CFT has Lorentzian signature, then its symmetry group is isometric to $SO(d+1, 2)$.

As in a (continuum) general quantum field theory one classifies states with respect to the symmetry elements of the Poincare group (translations and rotations), it is possible to introduce extra quantum numbers with the additional symmetries. Under translation and rotations a scalar operator transforms as

$$[P_\mu, \mathcal{O}(x)] = i\partial_\mu \mathcal{O}(x), \quad (1.47)$$

$$[L_{\mu\nu}, \mathcal{O}(x)] = -i(x_\mu \partial_\nu - x_\nu \partial_\mu) \mathcal{O}(x). \quad (1.48)$$

In a CFT the most important quantum number is the scaling dimension of the operator. A trivial example of a CFT is a massless, free scalar field. In this case the fundamental field ϕ is a primary operator (for $d > 1$) and its 'naive' dimension (the one we can deduce from the Lagrangian) and 'true' scaling dimension (the one appears in the propagator) are the same. In an interacting theory, this is not the case however. Therefore we will always mean the latter by scaling dimension. On the other hand there are special operators for which the scaling dimension does not renormalize even in a strongly interacting theory. In some examples this phenomenon is highly specific to the concrete theory i.e. in supersymmetric theories where the protection is due to supersymmetry. However, it is generic that the energy momentum tensor $T_{\mu\nu}$ and a global current J_μ possess the 'naive' dimensions due to their conservation laws. In d dimensions it means $\Delta_T = d + 1$, $\Delta_J = d$.

If the scaling dimension of \mathcal{O} is Δ at the fixed point, its commutator with the dilatation operator is

$$[D, \mathcal{O}(0)] = i\Delta \mathcal{O}(0). \quad (1.49)$$

We have one more generator: the one of the special conformal transformations. By definition, we call \mathcal{O} a primary operator if it satisfies the commutation relation

$$[K_\mu, \mathcal{O}(0)] = 0. \quad (1.50)$$

There are also operators which have definite scaling quantum numbers but are not primaries. For example, if \mathcal{O} is primary, then its derivatives

(for example $\partial_\nu \mathcal{O}$) are not. To see this, first we write the commutation relations (1.49), (1.50) for a general point x :

$$[D, \mathcal{O}(x)] = i (\Delta + x^\mu \partial_\mu) \mathcal{O}(x), \quad (1.51)$$

$$[K_\mu, \mathcal{O}(x)] = i \left(2x_\mu \Delta + 2x_\mu (x^\rho \partial_\rho) - x^2 \partial_\mu \right) \mathcal{O}(x). \quad (1.52)$$

If we differentiate these two properties, we can see that $\partial_\nu \mathcal{O}$ satisfies (1.49) with $\Delta_{\partial \mathcal{O}} = \Delta_{\mathcal{O}} + 1$. However, the commutator with K_μ is not of the form of (1.50)

$$[K_\mu, \partial_\nu \mathcal{O}(0)] = 2i \eta_{\mu\nu} \Delta \mathcal{O}(0) \neq 0. \quad (1.53)$$

Derivatives of a primary are called descendants and together with the primary operators they span the space of possible local operators. An important theorem of the field of conformal field theories is that states in the theory are in one-to-one correspondence with local operators. Therefore primary and descendant states also span the Hilbert space of the system.

The conformal symmetry has large implications for the form of correlation function in a CFT. We can concentrate on correlation function of primary operators, since every other quantities follows from them. For a primary \mathcal{O}_1 and \mathcal{O}_2 with conformal dimension Δ_1 and Δ_2 the two point function has the scaling form

$$\langle \mathcal{O}_1(x) \mathcal{O}_2(y) \rangle = \frac{1}{|x-y|^{2\Delta_1}} \delta_{\Delta_1, \Delta_2}. \quad (1.54)$$

The form of the three-point function of primary operators are also fixed by the conformal symmetry. Let us consider the \mathcal{O}_1 , \mathcal{O}_2 and \mathcal{O}_3 with dimensions Δ_1 , Δ_2 , Δ_3 . It turns out that the combinations

$$\alpha_{ijk} = \frac{\Delta_i + \Delta_j - \Delta_k}{2}, \quad (1.55)$$

where $i, j, k = 1, 2, 3$, determines the powers in the form of the three-point function in the following way:

$$\langle \mathcal{O}_1(x_1) \mathcal{O}_2(x_2) \mathcal{O}_3(x_3) \rangle = \frac{\lambda_{123}}{(x_{12})^{2\alpha_{123}} (x_{13})^{2\alpha_{132}} (x_{23})^{2\alpha_{231}}} \quad (1.56)$$

with $x_{ij} = x_i - x_j$.

Finally, for a four point function, conformal invariance cannot fix the form of momentum dependence completely, but it still restricts it. Taking

only one type of operator with conformal dimension Δ one can arrive to the formula

$$\langle \mathcal{O}(x_1) \mathcal{O}(x_2) \mathcal{O}(x_3) \mathcal{O}(x_4) \rangle = \frac{1}{(x_{12})^{2\Delta} (x_{34})^{2\Delta}} F(u, v), \quad (1.57)$$

where F is an arbitrary function which depends in the conformal cross ratios

$$u = \frac{x_{12}^2 x_{34}^2}{x_{13}^2 x_{24}^2} \quad (1.58)$$

$$v = \frac{x_{14}^2 x_{23}^2}{x_{13}^2 x_{24}^2}. \quad (1.59)$$

Large- N CFTs and generalized free field theory

So far we have introduced two type of systems in which one can use non-perturbative methods: large- N theories and conformal field theories. In the former one has a large number of degrees of freedom per spacetime point which suppress 'quantumness' compare to system with a few degrees of freedom. In the latter one can use the large symmetry group to gain information about the correlation functions.

A natural question arises: what happens if we combine these two properties and consider large- N CFTs. We will focus on matrix type theories since we have seen that they are richer in the large- N limit. These systems first appeared in the study of supersymmetric gauge theories where due to supersymmetry (another symmetry which we can use for studying strongly coupled physics) one can analyze RG flows and fixed point structures non-perturbatively. We will review $\mathcal{N} = 4$ super Yang-Mills theory, the most symmetric field theory that exists in physics in Section 1.3. This is a very special system originally studied by string theorists and mathematical physics but it has become relevant in a much wider range of applications since the discovery of AdS/CFT and holography.

Let us put together what we know about correlation functions in a large- N CFT. The most important objects here are single trace primary operators. From large- N considerations we have seen that the higher-point correlation functions at leading order are gaussian. The two-point function, however, is not constrained and has the form of (1.54) with non-trivial scaling dimensions Δ . Because of these properties (non-trivial two-point but gaussian higher-point correlator) at infinite N we call these theories generalized free field (or generalized mean field) theories.

We also know more about the Hilbert space structure of the CFT at large N . If \mathcal{O} is a single trace primary with conformal dimension Δ , then \mathcal{O}^2 is a multitrace primary with dimension 2Δ . Taking another example, it can be shown by differentiating (1.52) that $\partial_\nu \mathcal{O} \mathcal{O} - \mathcal{O} \partial_\nu \mathcal{O}$ is also primary with dimension $2\Delta + 1$. In general we can construct a whole new tower of primaries by sandwiching differential operators between two copies of \mathcal{O} with the schematic form of

$$[\mathcal{O}\mathcal{O}]_{n,l} \sim \mathcal{O} \left(\overleftrightarrow{\partial} \right)^{2n} \overleftrightarrow{\partial}_{\mu_1} \dots \overleftrightarrow{\partial}_{\mu_n} \mathcal{O}. \quad (1.60)$$

Due to large- N its dimension is the naive $\Delta(n, l) = 2\Delta + 2n + l$. However at finite N this gets corrected leading to an anomalous dimension $\gamma(n, l)$. These operators will play a crucial role in the interpretation of the results in Chapter 2.

1.3 AdS/CFT

In this section we will introduce probably the most exciting discovery of theoretical physics which connects many research areas. AdS/CFT (or holographic duality in general) is rooted in string theory. However, to motivate its results we will use the knowledge we introduced in the previous sections. AdS/CFT states the equivalence between certain quantum field theories in D dimensional flat space-time and quantum gravity in curved background in one dimension higher. Therefore from a fundamental physics point of view it gives us the possibility to study quantum gravity from perspective we are more familiar.

The AdS/CFT correspondence, however, has a very important feature which makes it even more remarkable and interesting for a wider range of audience. It is a weak-strong duality in the sense that when the gravity side is weakly coupled, the field theory is strongly coupled. This means that by studying weakly coupled gravitational systems we can deduce properties of strongly correlated ones.

In practice there are limitations of this method. Most notably, we understand this duality well for matrix large- N theories only. Moreover, in the cases where we do know the two sides in details, the field theories are close to QCD but very different from other areas of physics such as the condensed matter systems. However, even if we do not know the exact Lagrangian of the field theory (which in the case of strong coupling are

much less informative than in perturbative physics) this method can be very insightful about universal features.

Let us summarize the content of the original correspondence found in 1997 by Juan Maldacena [5]. The field theory consist $\mathcal{N} = 4$ super Yang-Mills theory in four space-time dimensions. \mathcal{N} denote the number of generators of supersymmetry the system has. In flat space this corresponds to the largest supersymmetry group. This is actually so restrictive that it determines not only the total field content but also the interaction structure of the theory. The fields are:

- A_μ non-Abelian gauge field of some gauge group (say $SU(N)$)
- Four species of fermions ψ^a , where $a = 1, \dots, 4$ is the flavor index
- Six scalar fields X_i $i = 1, \dots, 6$

The Lagrangian of the theory has the form

$$\mathcal{L}_{SYM} = -\frac{1}{4g_{YM}^2} Tr \left[F_{\mu\nu} F^{\mu\nu} + D_\mu X^i D^\mu X^i + \bar{\psi}^i \gamma^\mu D_\mu \psi^i + [X^i, X^j]^2 + \dots \right], \quad (1.61)$$

where ... indicates Yukawa type of interactions between the scalars and fermions. These are necessary for supersymmetry.

This theory seems very complicated in terms of field content and interactions. However, this complicated structure results a very important simple observation. This theory has a vanishing β function for all value of g_{YM} . This feature has such important consequences in the properties of physical observables such as scattering amplitudes that it is reasonable to say that actually $\mathcal{N} = 4$ SYM is one of the simplest quantum field theory [40].

Maldacena conjectured that the theory above is equivalent to type IIB string theory living in the spacetime of $AdS_5 \times S_5$. Here S_5 denotes the five-dimensional sphere and AdS_5 is an Anti-de-Sitter spacetime which properties will be discussed shortly. This theory can be characterised by a number of parameters. In string theory we have a length parameter which describes the tension of the string (l_s), and a coupling constant g_s which is the strength of the interaction between different strings. Additionally, the AdS_5 background has a length scale L . The connection of the parameters between the two sides are:

$$4\pi g_s = g_{YM}^2 = \frac{\lambda}{N}, \quad (1.62)$$

$$\frac{L}{l_s} = \lambda^{1/4}, \quad (1.63)$$

where $\lambda = g_{YM}^2 N$ is the t'Hooft coupling of the $\mathcal{N} = 4$ SYM theory.

This immediately shows two limits which can be taken in order to obtain a tractable duality. First of all the large- N limit $\lambda \ll N$ suppresses quantum gravity effects (which corresponds to small g_s). Also, to work with only supergravity fields (low energy mode of the string) instead of the entire string spectrum then we can take L/l_s large. This corresponds to the large t'Hooft coupling limit in the field theory. Note, that since we do not have a well established theory of non-perturbative strings, considering large N is crucial. It is, however, in principle possible to move away from the supergravity limit.

This prototype of holographic duality is very well tested in details. We will see that scaling dimensions in the field theory side correspond to the spectrum in the string theory. In the strongly coupled $\mathcal{N} = 4$ SYM theory there are special single trace operators, whose scaling dimensions can be determined with the help of integrability. These have been compared to the weakly coupled string theory spectrum and a perfect agreement was found [39].

1.3.1 AdS spacetime

To present the more general content of the correspondence let us study the structure of AdS spacetime. Specifically we will present two useful sets of coordinates: the global coordinates and the Poincare patch. In the former, the symmetries of the system are more manifest and it is useful when one is studying general features of the duality. The latter, however, is used more often in practical calculations and applications.

First, however let us make some coordinate independent remarks on AdS. This spacetime is a solution of the vacuum Einstein's equation with negative cosmological constant

$$R_{\mu\nu} - \frac{1}{2}g_{\mu\nu}(R - 2\Lambda) = 0. \quad (1.64)$$

By taking the trace of the equation (in Lorentzian signature) one can see that the curvature (Ricci scalar) is constant throughout the entire spacetime

$$R = \frac{2D}{D-2}\Lambda. \quad (1.65)$$

AdS has constant negative curvature and therefore it can be obtained by embedding a hyperboloid in a $D + 1$ dimensional flat space with signature $(-, -, +, +, \dots)$

$$X_0^2 + X_{d+2}^2 - \sum_{i=1}^{d+1} X_i^2 = L^2, \quad (1.66)$$

where $d = D - 2$ is the number of spacelike directions in our original spacetime and the AdS radius L is related to the Ricci curvature by

$$L^2 = -\frac{D(D-1)}{R}. \quad (1.67)$$

The solution of the constraint (1.66) can be parametrized in the following way

$$\begin{aligned} X_0 &= L \frac{\cos \tau}{\cos \rho}, \\ X_{d+2} &= L \frac{\sin \tau}{\cos \rho}, \\ X_i &= Lu_i \tan \rho. \end{aligned} \quad (1.68)$$

Here $\tau \in (-\infty, \infty)$ is a timelike coordinate, $\rho \in [0, \pi/2)$ is a spacelike compact coordinate and u_i $i = 1, \dots, d + 1$ are the component of a unitvector. With these coordinates the AdS metric can be deduced from the induced metric formula $g_{ab} = \partial_a X^\mu \partial_b X^\nu \eta_{\mu\nu}^{(2)}$, where $\eta_{\mu\nu}^{(2)}$ is the flat space metric with signature $(-, -, +, +, \dots)$. The result is

$$ds^2 = \frac{L^2}{\cos^2 \rho} \left(-dt^2 + d\rho^2 + \sin^2 \rho d\Omega_d^2 \right). \quad (1.69)$$

This shows that AdS is conformally equivalent to a cylinder as in Fig. 1.11. The global time coordinate runs parallel to the axis of the cylinder while ρ is the radial coordinate. The conformal boundary is at $\rho = \pi/2$. Note that although the coordinate ρ terminates at a finite value, the boundary is still infinitely far away from an arbitrary point with $\rho < \pi/2$ due to the conformal $1/\cos^2 \rho$ factor in the metric.

An alternative way of parametrizing (part of) AdS space is with the

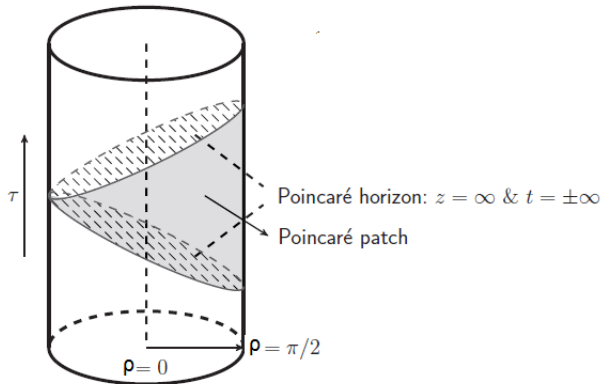


Figure 1.11. AdS spacetime and its parametrization with global coordinates and Poincaré Patch coordinates in lorentzian signature. The shaded area indicates the region what the Poincaré Patch covers (from [8]).

Poincaré coordinates (t, \vec{x}, z) :

$$\begin{aligned}
 X_0 &= \frac{z}{2} \left(1 + \frac{L^2 + \vec{x}^2 - t^2}{z^2} \right) \\
 X_{d+2} &= \frac{L}{z} t \\
 X_{i < d+1} &= \frac{L}{z} x_i \\
 X_{d+1} &= \frac{z}{2} \left(-1 + \frac{L^2 - \vec{x}^2 + t^2}{z^2} \right), \tag{1.70}
 \end{aligned}$$

where $z \in (0, \infty)$ is the radial coordinate and $x_i, t \in (-\infty, \infty)$ are very similar to Cartesian coordinates in flat space. With these coordinates the metric takes the form

$$ds^2 = \frac{L^2}{z^2} \left(-dt^2 + dz^2 + \sum_{i=1}^d dx_i^2 \right). \tag{1.71}$$

An often used form of the metric (1.71) uses instead of z the radial coordinate we use $r = L^2/z$:

$$ds^2 = \frac{r^2}{L^2} \left(-dt^2 + d\vec{x}^2 \right) + \frac{L^2}{r^2} dr^2. \tag{1.72}$$

In this parametrization, $r = \infty$ is the position of the boundary.

It is important to note that in Lorentzian signature the Poincare patch only covers a part of global AdS. This can be seen by expressing t from (1.68) and (1.70)

$$t = L \frac{\sin \tau}{\cos \tau - u_{d+1} \sin \rho}.$$

The limit $t \rightarrow \pm\infty$ corresponds to the case where the denominator vanishes which happens at finite value of τ .

The Euclidean version of the metric can be obtained by flipping the sign of the timelike coordinate. The relation between the embedding coordinates and the global coordinates are (1.68) with $\sin \tau \rightarrow \sinh \tau$ and $\cos \tau \rightarrow \cosh \tau$. Note also, that in this case the Poincare Patch covers the whole AdS spacetime.

AdS spacetime has a boundary related to the limit $\rho \rightarrow \pi/2$. This limit can be approached however in different ways. If we let $\rho \rightarrow \pi/2$ by keeping the other global coordinates (τ, Ω) fixed, we define a boundary surface with the topology of a sphere S_{D-1} . On the other hand, if we let the Poincare coordinate $z \rightarrow 0$ we arrive to a surface with flat metric and topology. Of course this later scaling can be also done in the global coordinates. To achieve this, in the case of Euclidean signature we have to take the limit $\epsilon \rightarrow 0$

$$\rho = \frac{\pi}{2} - \epsilon e^{-\tau}. \quad (1.73)$$

In this case, the metric in the boundary surface is

$$ds^2 = \frac{1}{\cos^2 \rho} \left(d\tau^2 + \sin^2 \rho d\Omega^2 \right) \rightarrow e^{2\tau} \left(d\tau^2 + d\Omega^2 \right) = dr^2 + r^2 d\Omega^2, \quad (1.74)$$

where $r = e^\tau$. We obtain therefore the flat metric in polar coordinates. The most important property of AdS_D spacetime is that its isometry group (in Euclidean signature) is $SO(D, 1)$. Therefore, the isometries of AdS are in one-to-one correspondence with the symmetries of a CFT in lower dimensions.

1.3.2 The dictionary

In the previous section we have already mentioned that the symmetries of a CFT in flat space and the isometries of curved AdS space-time are identical. This indicates that we have two different descriptions of the same physics. We now turn to the detailed dictionary between the two theories.

Since the Hilbert space of the two system is identical according to the conjecture, their partition function must be equal:

$$Z_{CFT}(N) = Z_{AdS}(N) = \int \mathcal{D}\phi \exp\left(iN^2 S_{AdS}(\phi)\right). \quad (1.75)$$

On the right-hand side ϕ is the set of all fields living in AdS . We explicitly indicated the N dependence in the exponent. In case of large- N we can approximate the path integral by its saddle point. In fact, it is the only limit where our correspondence is tractable.

The most important dictionary element is the rule to compute correlation functions for the field theory. This is called the Gubser-Klebanov-Polyakov-Witten (GKPW) rule after its inventors [6, 7]. Strictly speaking, this has a conjectural status (as everything else in holography) but it passed numerous non-trivial tests.

First, let us recall that a correlation function in field theory can be calculated by modifying the Lagrangian by adding source terms in the form:

$$\mathcal{L}(x) \rightarrow \mathcal{L}(x) - i \sum_i j_i(x) \mathcal{O}_i(x). \quad (1.76)$$

Having done this, one can compute any correlation function by first calculating the log of the partition function of the theory in the presence of the external sources $Z[J_i]$ and using the formula:

$$\langle \mathcal{O}_1(x_1) \mathcal{O}_2(x_2) \dots \mathcal{O}_n(x_n) \rangle = \prod_{i=1}^n \frac{\delta}{\delta j_i(x_i)} \log Z_{CFT}|_{j=0}. \quad (1.77)$$

The question is how to generalize (1.75), or in other words what the sources on the field theory side correspond to in the gravitational theory. The answer turns out to be somewhat counterintuitive: the sources in the field theory translate to a boundary condition for the fields ϕ in AdS . (1.75) generalizes to

$$Z_{CFT}[j] = \langle e^{\int d^{d+1}x j(x) \mathcal{O}(x)} \rangle_{CFT} = \int \mathcal{D}\phi e^{iN^2 S_{AdS}(\phi(x,r))|_{\phi(x,r=\infty)=j(x)}}, \quad (1.78)$$

where r is the radial coordinate with the property that the boundary is at $r = \infty$. As we discussed, in practice we choose N to be large so that we can approximate (1.78)

$$\int \mathcal{D}\phi e^{iN^2 S_{AdS}(\phi(x,r))|_{\phi(x,r=\infty)=j(x)}} \sim e^{iN^2 S_{on-shell}(\phi(x,r))|_{\phi(x,r=\infty)=j(x)}}. \quad (1.79)$$

To calculate a specific correlation function we need to go through the following steps. First we solve the classical equation of motions with general boundary conditions $\phi(\partial_{Bulk})$. Then, this is substituted into S_{AdS} to obtain the on-shell action. Finally, according to (1.77), we differentiate (1.79) with respect to the boundary conditions.

There is one important detail in the above procedure which we did not touch upon. By considering the integral of the whole spacetime, the on-shell action $S_{on-shell}$ turns out to be infinite. To cure this divergence, we need to regularize our theory by cutting off the spacetime and place the boundary at a finite $r_{cutoff} = \epsilon^{-1}$ radius (instead having it at infinity). This property of the gravitational theory is actually not a surprise. The dual quantum field theory (as the majority of interacting QFTs) is expected to have UV divergencies. These divergences can be shown to translate to the infinite bulk action due to the infinite volume of AdS. This is one of the clearest examples of an aspect of AdS/CFT known as UV-IR duality because the cutoff r_{cutoff} is an IR regulator in the bulk. As in normal QFT the choice of regularization can be fixed by adding counterterms to the bulk action. To address these questions, a systematic treatment for a general class of spacetimes was developed under the name of holographic renormalization [42].

As the most elementary example let us take a massive scalar field in euclidean AdS with the action:

$$S = \frac{1}{2} \int d^{d+1}x dr \sqrt{g} \left(\partial_\mu \phi \partial^\mu \phi + m^2 \phi^2 \right), \quad (1.80)$$

By applying the GPKW rule to this case one obtains for the (boundary) 2-point function:

$$\langle \mathcal{O}(\vec{x}_1) \mathcal{O}(\vec{x}_2) \rangle = \frac{C_1}{|\vec{x}_1 - \vec{x}_2|^{2\Delta}}, \quad (1.81)$$

where C_1 is a constant and the power Δ denotes the combination

$$\Delta = \frac{d+1}{2} + \sqrt{\frac{(d+1)^2}{4} + m^2 L^2}. \quad (1.82)$$

We can see that the result (1.81) has the scaling form (1.54) indicating that the dual field theory is a CFT.

To further verify this we can check the three-point function. For this, we need to introduce an interaction term in the bulk action:

$$S_{int} = \int d^{d+2}x \sqrt{g} \left(\frac{\lambda}{3!} \phi^3 \right). \quad (1.83)$$

The result of the holographic calculation has the form:

$$\langle \mathcal{O}(\vec{x}_1) \mathcal{O}(\vec{x}_2) \mathcal{O}(\vec{x}_3) \rangle = \frac{C_2}{|\vec{x}_1 - \vec{x}_2|^\Delta |\vec{x}_1 - \vec{x}_3|^\Delta |\vec{x}_2 - \vec{x}_3|^\Delta}, \quad (1.84)$$

with the coefficient C_2 being proportional to the coupling λ . This is also consistent with the CFT result (1.56). The relations (1.82) and (1.84) are crucial results. They tell us how to relate the conformal dimensions and OPE coefficients of an operator (which are boundary data) to the mass and coupling parameters in the bulk. It is also important to note that the above form of correlation functions implies that the operators in the CFT which have dual fields in the bulk are single trace primary operators.

We will shortly see that the GPKW rule extends to correlation functions of operators with more non-trivial index structure, such as $\langle T_{ij}(\vec{x}_1) J_k(\vec{x}_2) J_l(\vec{x}_2) \rangle$ (with T and J being the energy-momentum tensor and the conserved current respectively). These were computed in e.g. [41]. Again, the conformal symmetry allows one to determine the complex structure of this correlator and the holographic result is in perfect agreement.

As we mentioned, the GPKW rule is a bit counterintuitive. In many cases, it effectively reduces to a simpler prescription that gives the same results. Let us consider the correlation function of a scalar living in AdS spacetime with the action (1.80) (plus possible interactions such as (1.83)) $\langle \prec(\vec{x}_1, r_1) \dots \prec(\vec{x}_n, r_n) \rangle_{AdS}$. For example, the two point function (called also the bulk-to-bulk propagator) is the Green's function of the free equation of motion in AdS

$$\left(\nabla^\mu \nabla_\mu - m^2 \right) \mathcal{G}(x_1, r_1; x_2, r_2) = \frac{1}{\sqrt{g}} \delta^{d+1}(x_1 - x_2) \delta(r_1 - r_2). \quad (1.85)$$

We can obtain a correlation function in the boundary theory by considering the corresponding bulk n -point function and taking the radial coordinates r to the boundary while rescaling the expression it in the following way:

$$\langle \mathcal{O}(\vec{x}_1) \dots \mathcal{O}(\vec{x}_n) \rangle \sim \lim_{r_1, \dots, r_n \rightarrow \infty} r_1^\Delta \dots r_n^\Delta \langle \prec(\vec{x}_1, r_1) \dots \prec(\vec{x}_n, r_n) \rangle_{AdS}. \quad (1.86)$$

Although this method is more intuitive (and in some situation can be quicker way to calculate), the GPKW rule is easier to use if one consider non-conformal theories such as models with finite temperature and density.

1.3.3 Finite density and temperature

For most of the interesting systems in condensed matter physics the conformal symmetry is broken by several scales. The usefulness of AdS/CFT in applications originates from the fact that the original correspondence can be deformed in many ways. Specifically, we are often interested in systems at finite temperature and chemical potential. Let us summarize here how to incorporate these effects.

For the dual description of a chemical potential we need to first describe, how a $U(1)$ global conserved current J_μ translates into the bulk theory. Because it obeys the conservation law $\partial_\mu J^\mu = 0$, its conformal dimension is fixed to the canonical dimension which is $\Delta_J = d$ as we mentioned in Section (1.2.2). Furthermore, in the bulk, the corresponding field has to be a vector field. There is a slightly different analog of (1.82) which relates the conformal dimension and the mass in case of the spin-1 field which dictates that our dual vector field has to be massless. In other words it has to be invariant under gauge transformation so its action is fixed to usual Maxwell term:

$$S_A = -\frac{1}{4g_F^2} \int d^{d+1}x dr F^{\mu\nu} F_{\mu\nu}, \quad (1.87)$$

with $F_{\mu\nu} = \nabla_\mu A_\nu - \nabla_\nu A_\mu$. Interestingly, a global symmetry in the boundary translates into a local symmetry in the bulk.

A chemical potential μ means that we deform our original theory by $\delta S = \mu Q = \mu \int d^{d+1}x J^0(x)$. By looking at (1.78) with the specific deformation of $j(x) = \mu$, $\mathcal{O}(x) = J^0(x)$ we can see that solving our bulk theory with the boundary condition $A_0(r \rightarrow \infty) = \mu$ corresponds to a boundary theory at finite density.

We can identify the dual of the energy-momentum tensor by similar logic. Its conformal dimension is also equal its canonical dimension $\Delta_T = d + 1$ as it is also a conserved current $\partial_\mu T^{\mu\nu} = 0$. This again results a masslessness condition for the spin-2 dual tensor field. However, the only consistent theory of interacting massless spin-2 fields is general relativity, therefore the dual field must be the metric tensor $g_{\mu\nu}$ itself. As a result, by studying the fluctuations of the metric (gravitational waves) in the bulk one can gain information about the energy and momentum dynamics.

So far in our introduction to AdS/CFT we have been discussing zero temperature physics. One of the most remarkable fact of AdS/CFT how naturally it can encode finite temperature systems. This is done by changing the bulk geometry so that it includes black holes. To see this, let us

write down the asymptotically AdS black hole solution (or black brane more precisely) with planar horizon (which is similar to the Schwarzschild solution in asymptotically flat space):

$$ds^2 = \frac{r^2}{L^2} \left(f(r) d\tau^2 + \sum_{i=1}^d dx_i^2 \right) + \frac{L^2}{r^2 f(r)} dr^2, \quad (1.88)$$

with

$$f(r) = 1 - \frac{r_H^{d+1}}{r^{d+1}}, \quad (1.89)$$

where r_H is the position of the horizon of the black hole. The Hawking temperature of this black hole can be determined by the following argument. The solution (1.88) is plagued by an unphysical conical defect unless we make the (imaginary) time direction τ periodic ($\tau \sim \tau + \beta$) with the period

$$\beta = \frac{4\pi L^2}{r_H^2 f'(r_H)} = \frac{4\pi L^2}{(d+1)r_H}. \quad (1.90)$$

In the boundary field theory the time direction is identified with τ in the bulk and therefore it is also periodic. However, in thermal field theory a periodic imaginary time means that our system is considered in a heat bath with a temperature equal to the inverse of the time period:

$$T = \frac{(d+1)r_H}{4\pi L^2}. \quad (1.91)$$

This temperature in the dual CFT is thus given by the Hawking temperature of the bulk AdS black hole [11]. We can of course reverse this thought process and for a specific temperature T we can choose a horizon position r_H to describe the dual gravitational system.

Usually, we are interested in systems which are at finite temperature and density at the same time. For this we need to combine the two descriptions and this calls for the black hole solutions of the Einstein-Maxwell action

$$S_{EM} = \int d^{d+2}x \sqrt{g} \left[\frac{1}{16\pi G} \left(R + \frac{d(d+1)}{L^2} \right) - \frac{1}{4g_F^2} F_{\mu\nu} F^{\mu\nu} \right], \quad (1.92)$$

with the boundary condition $A_0(r \rightarrow \infty) = \mu$. The solution for the metric is still in the form of (1.88) but with the emblackening factor

$$f_{RN}(r) = 1 + \frac{Q^2}{r^{2d}} - \frac{M}{r^{d+1}}, \quad (1.93)$$

where Q and M are the charge and mass of the black hole. The gauge field profile in this solution is

$$A_0 = \mu \left(1 - \frac{r_H^{d-1}}{r^{d-1}} \right). \quad (1.94)$$

This black hole, the charged Reissner-Nordstrom (RN) black hole, has two horizons in general but for us only the outer one (at position r_H) has importance. The relation between its position and the parameters of the black hole can be determined from the condition $f_{RN}(r_H) = 0$:

$$M = r_H^{d+1} + \frac{Q^2}{r_H^{d-1}}. \quad (1.95)$$

For studying a boundary theory at temperature T and chemical potential μ we need to choose the mass and the charge such that

$$T = \frac{(d+1)r_H}{4\pi L^2} \left(1 - \frac{(d-1)Q^2}{(d+1)r_H^{2d}} \right), \quad (1.96)$$

$$\mu = \frac{g_F Q}{2c_d \sqrt{\pi G} L^2 r_0^{d-1}}, \quad (1.97)$$

with

$$c_d = \sqrt{\frac{2(d-1)}{d}}. \quad (1.98)$$

This solution is especially interesting in the limit where the temperature goes to zero but the chemical potential is fixed. In this extremal limit the two separate horizons mentioned above merge and form a double horizon despite the fact that we are in zero temperature. It means that near the horizon the embleckening factor takes the form

$$f_{NH}(r) = d(d+1) \frac{(r-r_H)^2}{r_H^2} + \dots \quad (1.99)$$

We can see the double zero of $f_{NH}(r)$ from this expression. If we define new near horizon variables

$$L_2 = \frac{L}{\sqrt{d(d+1)}}, \quad (1.100)$$

$$\zeta = \frac{L_2}{r - r_H} \quad (1.101)$$

then the near horizon metric can be written as

$$ds^2 = \frac{L_2^2}{\zeta^2} (d\tau^2 + d\zeta^2) + \frac{r_H^2}{L^2} \sum_{i=1}^d dx_i^2. \quad (1.102)$$

Comparing to the *AdS* metric in the coordinates (1.71) we recognize that here the space time is a product of two dimensional Anti-de-Sitter space and flat space resulting in the geometry of $AdS_2 \times \mathbb{R}^d$.

This is a remarkable result and has profound implication to the boundary field theory. According to holography, the radial direction can be thought of a flow of the renormalization group such that the UV of the field theory is characterized by the near boundary geometry and the IR is characterized by the near horizon geometry. Let us study the scaling properties of the UV and IR limit. The UV geometry is invariant under the relativistic, $\mathbf{z} = 1$ scaling

$$\tau \rightarrow s\tau, \quad z \rightarrow sz, \quad \mathbf{x} \rightarrow s\mathbf{x}, \quad (1.103)$$

while the IR $AdS_2 \times \mathbb{R}^2$ is invariant under

$$\tau \rightarrow s\tau, \quad \zeta \rightarrow s\zeta, \quad \mathbf{x} \rightarrow \mathbf{x}. \quad (1.104)$$

Comparing this with the general form of (1.16) we can see that the IR of the theory has the dynamical critical exponent of $\mathbf{z} = \infty$.

The extremal RN geometry therefore corresponds to a flow from a CFT with $\mathbf{z} = 1$ to a state with $\mathbf{z} = \infty$ upon turning on a chemical potential. This property is called “local quantum criticality” since only the time direction has scaling behavior.

The question arises whether it is possible to construct holographic examples with more general \mathbf{z} . The answer turns out to be yes, but for this we need to consider slightly more general models. The hint comes from the string theoretical construction of *AdS/CFT*. Generally, in a top-down construction there are numerous fields living in *AdS* but most of them have large masses so we can ignore them. However, there is a type of field which generically appears in the low-energy spectrum called the dilaton field. It is a scalar similar to the example above but it has unusual properties from a traditional field theory point of view. Namely it has non-linear and non-minimal coupling to the gauge field. The extended

theory is the ‘‘Einstein-Maxwell-dilaton’’ gravity [37, 36, 38, 35] with the Lagrangian

$$\mathcal{L} = R - \frac{1}{2}(\partial_\mu\phi)^2 - \frac{Z(\phi)}{4}F^2 - V(\phi). \quad (1.105)$$

We can think of this as modification of the pure ‘‘Einstein-Maxwell’’ theory that makes the gauge coupling dynamical $g_{F,eff} = Z^{-1}(\phi)$. This generalization is parametrized by two functions: $V(\phi)$ and $Z(\phi)$. Based on string theory arguments these are usually approximated by the exponential forms: $V(\phi) \sim e^{\alpha_2\phi}$ and $Z(\phi) \sim e^{\alpha_1\phi}$.

After solving the Einstein’s equation for this type of theory, the IR metric (near $r = 0$) can be written in the following form

$$ds_{EMD}^2 = r^{-2\theta/d} \left(r^{2\mathbf{z}} d\tau^2 + r^2 dx_i^2 + \frac{dr^2}{r^2} \right) + \dots, \quad (1.106)$$

with

$$\theta = \frac{d^2\alpha_2}{\alpha_1 + (d-1)\alpha_2}, \quad \mathbf{z} = 1 + \frac{\theta}{d} + \frac{2(d(d-\theta) + \theta)^2}{d^2(d-\theta)\alpha_1}. \quad (1.107)$$

We have a family of solution with two parameters. We do not touch upon the parameter θ here which is called the hyperscaling violation exponent and we set it to zero for our discussion (we choose $\alpha_2 = 0$). In this special case the metric (1.106) is the so-called Lifshitz solution, which is invariant under the scale transformation

$$\tau \rightarrow s^{\mathbf{z}}\tau, \quad r \rightarrow s^{-1}r, \quad \mathbf{x} \rightarrow s\mathbf{x}. \quad (1.108)$$

This means that the boundary field theory has the dynamical critical exponent \mathbf{z} .

1.3.4 Holographic fermions

So far we have been investigated holographic models in which the bulk action contains only bosonic fields. Now, we briefly study here the exciting case where the bulk contains fermions as well. In the field theory side these correspond to fermionic single trace operators, e.g. $\mathcal{O}_\Psi \sim Tr(\phi\psi)$, where ϕ and ψ are bosonic and fermionic fundamental fields. The latter is quite natural from the perspective of the original correspondence since there the field theory is supersymmetric.

To study the properties of the fermion we need to incorporate the Dirac term into the gravitational action

$$S = \int d^{d+2}x \sqrt{-g} \left[\frac{1}{16\pi G} (R - 2\Lambda) - \frac{1}{4g_F^2} F_{\mu\nu} F^{\mu\nu} \right. \quad (1.109)$$

$$\left. - i\bar{\Psi} \left(e_a^\mu \Gamma^a \left(\partial_\mu + \frac{1}{4} \omega_{\mu bc} \Gamma^{bc} - iqA_\mu \right) - m \right) \Psi \right], \quad (1.110)$$

where Γ^a are the gamma matrices, e_a^μ is the so-called vielbein defined with the help of the flat metric η as $e_a^\mu e_b^\nu \eta_{ab} = g^{\mu\nu}$ and ω is the spin connection with the properties

$$\partial_\mu e_\nu^a - \Gamma_{\mu\nu}^\sigma e_\sigma^a + \omega_{\mu\nu}^a e_\nu^b = 0. \quad (1.111)$$

Here we have restricted ourself to a bulk action containing only the metric, the gauge field and the fermion field. A natural generalization of this involves the dilaton field introduced in the previous section.

Probe limit

Solving (1.110) in generality is a very hard task and one needs additional approximations. Fermions are intrinsically quantum mechanical objects and therefore in the large- N (semiclassical) limit their backreaction to the geometry and gauge field is small. A natural simplification is to consider the fermion dynamics in the fixed background determined by the other fields. We have seen in Section 1.3.3 that this background is the charged Reissner-Nordstrom (RN) black hole.

The most interesting quantity to compute is the Green's function of the fermionic operators in the boundary field theory. In general, this can only be done numerically as in the first papers on this topic [10, 9, 34]. Later, the problem was reconsidered in a semi-analytical approach which uses the AdS_2 nature of the IR geometry [33, 32].

The key step in this method is to determine the IR AdS_2 Green's function \mathcal{G} which is just the fermion retarded two-point function obtained using the $AdS_2 \times \mathbb{R}^2$ background (1.102) (we restrict ourselves to $d = 2$ dimensions). It has the form

$$\mathcal{G}_k(\omega) = c_k e^{i\phi_k} \omega^{2\nu_k}, \quad (1.112)$$

where c_k and ϕ_k are real, analytical function of the momenta k . The $\mathbf{z} = \infty$ local quantum critical scaling is manifest in the power law fre-

quency dependence. The exponent ν_k depends on the momentum, chemical potential and the parameters of the fermion (mass and charge):

$$\nu_k = \sqrt{\frac{2k^2}{\mu^2} + \frac{m^2}{6} - \frac{q^2}{3}}. \quad (1.113)$$

The full RN black hole geometry interpolates between the near horizon $AdS_2 \times \mathbb{R}^2$ and the near boundary AdS_4 region. It turns out by matching asymptotic expansions that the full Green's function G_R at low frequencies $\omega \ll \mu$ can be obtained from \mathcal{G} :

$$G_R(\omega, k) = \frac{b_+^{(0)} + \omega b_+^{(1)} + \mathcal{G}_k(\omega) (b_-^{(0)} + \omega b_-^{(1)})}{a_+^{(0)} + \omega a_+^{(1)} + \mathcal{G}_k(\omega) (a_-^{(0)} + \omega a_-^{(1)})}. \quad (1.114)$$

We ignored in the formula (real) terms of order ω^2 . The coefficients $a_{\pm}^{(i)}$, $b_{\pm}^{(i)}$ which can be determined numerically, are real functions of the momentum and the parameters of the model (chemical potential, mass and charge of the fermion). The realness of these coefficients implies that the spectral function is proportional to the AdS_2 spectral function in the limit $\omega \rightarrow 0$

$$A(\omega, k) = ImG_R(\omega, k) \sim Im\mathcal{G}_k(\omega) + \dots, \quad (1.115)$$

provided $a_+^{(0)} \neq 0$. This latter condition is satisfied when the mass to charge ratio m/q is large.

However, when m/q is small the coefficient $a_+^{(0)}$ can vanish linearly around a momenta k_F : $a_+^{(0)}(k) = v_F(k - k_F) + \dots$. In this case (1.114) can be written near k_F in the familiar form of (1.1):

$$G_R(\omega, k) \approx \frac{Z}{\omega - v_F(k - k_F) - \Sigma(\omega, k)} + \dots, \quad (1.116)$$

with the self-energy being of the form of

$$\Sigma(\omega, k) = -\frac{c_{k_F}}{a^{(1)}(k_F)} e^{i\phi_k} \omega^{2\nu_{k_F}} \sim \mathcal{G}_k(\omega). \quad (1.117)$$

The emergent parameters v_F and Z are functions of $a_{\pm}^{(i)}$ and $b_{\pm}^{(i)}$ evaluated at k_F .

We recognize parts of an interacting Fermion system as in the beginning but also very different. The value of the power $2\nu_{k_F}$ is a very important

in the behavior of our result. If $\nu_{k_F} > 1/2$, then at low frequencies the linear bare term dominates over the self-energy. It means that the system has well-defined quasiparticles whose lifetime however is different from quasiparticles in an ordinary Landau type Fermi-liquid (which has $\Sigma \sim \omega^2$). In the case of $\nu_{k_F} < 1/2$ we arrive to a novel non-Fermi liquid state without quasiparticles. In the special (finetuned) case of $\nu_{k_F} \rightarrow 1/2$ the self-energy has the marginal Fermi-liquid form $\Sigma \sim \omega \log \omega$ we have seen in formula (1.19). We see therefore that within this simple holographic model one can get a whole zoo of fermionic behavior with or without Fermi surfaces and quasiparticles, including models that we have only postulated phenomenologically up to this point.

Semi-holography

The result (1.117) that the self-energy is proportional to the AdS_2 propagator has a very insightful interpretation. It tells us that we are dealing with a nearly free fermion interacting with a matrix large- N local quantum critical system. To see this let us consider the following effective theory [48]. Let χ be the nearly free fermion and ψ a fermionic operator of a strongly coupled theory whose Green's function has the form $\langle \psi\psi \rangle = \mathcal{G}$. We then couple χ and ψ with the following (sometimes called semi-holographic) action:

$$S = S(\Psi) + \int dt d^d x \left(\chi^\dagger (i\partial_t - \epsilon(i\nabla) + \mu) \chi + g\chi^\dagger \Psi + g\Psi^\dagger \chi \right). \quad (1.118)$$

Here $S(\Psi)$ is the action for the strongly coupled system. We have seen that in the matrix large- N limit the higher-point correlators vanish. In this case the Dyson summation is exact for the χ fermion Green's function

$$\langle \chi^\dagger \chi \rangle = \sum_n g^n G_0 (\mathcal{G} G_0)^n = \frac{1}{G_0^{-1} + g\mathcal{G}}, \quad (1.119)$$

where G_0 denotes the free Green's function for the fermion χ . We obtained therefore a result from our effective action which has the same form as the fully holographic result.

One can qualitatively understand this structure by analysing in details the properties of the fermion wavefunction in the RN background. The region where the AdS_4 and $AdS_2 \times \mathbb{R}^2$ geometry meet can be thought as a domain wall where the fermion wavefunction localizes and interacts

weakly with its environment. However this fermion can tunnel to the near horizon local critical region. The latter therefore acts as a heat bath for the particle.

In this view of splitting the full system to a nearly free fermion and a local quantum critical subsystem our holographic setup has similarities to the Hertz-Millis type model in Section 1.1.4 used for the Ising-nematic transition. There the fermions however was coupled to a $\mathbf{z} = 1$ critical system, namely to a massless scalar. In view of the discussion there, the virtues and pitfalls of using AdS/CFT to study such theories should be clear. Nevertheless it is able to offer us novel insights into these complicated systems.

Instabilities

The above mentioned solutions for holographic fermions in the probe limit are very insightful but it turns out that in the parameter region where Fermi surfaces are found instabilities occur. The exponent of the AdS_2 Green's function (1.113) already signals this instability for the small m/q ratio. In that case ν_k become imaginary and \mathcal{G} shows log-oscillatory behaviour. It means that to quantitatively study these holographic systems with Fermi surfaces one needs to take into account the fermion backreaction to the geometry (and to the other fields). Determining the new geometry is a hard task and extra assumptions are needed to make the theory tractable. One approach is to approximate the fermions as a fluid and study the self-gravitating star-like objects and the geometry they have created [14]. This approximation turns out to be good if the total charge of the system Q is much larger than the individual charge q of a fermion. The crucial difference compare to the RN black hole geometry is the absence of a horizon.

Another crude approach is to by hand cut off the AdS geometry at some radial distance z_W and consider the fermions in this background. In this case we arrive by construction to a state which is an interacting CFT in the UV and a free Fermi gas in the IR. We will review this approach in the next chapter in details.

We end this section with table (1.1) summarizing our review of the basics of AdS/CFT by indicating the main dictionary elements.

Boundary field theory	Bulk gravitational theory
Partition function	Partition function
Scalar operator \mathcal{O}	Scalar field ϕ
Energy-momentum tensor $T_{\mu\nu}$	Metric $g_{\mu\nu}$
Current of a global symmetry J_μ	Gauge field A_μ
Fermionic operator \mathcal{O}_ψ	Dirac field ψ
Spin, charge of the operator	Spin, charge of the field
Conformal dimension of the operator	Mass of the field
Global space-time symmetry	Isometry of the geometry
Global internal symmetry	Local (gauge) symmetry
Finite temperature T	Black hole with Hawking temperature T
Chemical potential μ	Boundary condition for the gauge field $A_0(r \rightarrow \infty) = \mu$
RG flow	Evolution in the radial direction

Table 1.1. (Non-complete) dictionary for holography.

1.4 This thesis

In the rest of this thesis we apply these techniques to problems in strongly correlated physics. Chapter 2, 3 and 4 are based on the research papers [14–16] respectively.

In Chapter 2 we study pairing induced superconductivity in large N strongly coupled systems at finite density using holographic methods described in the previous section. The goal of this direction is to understand the pairing instability occurring in non-Fermi liquids. We made the first step by studying the pairing of a holographic Fermi liquid (Fermi liquid which is an interacting CFT in the UV). To obtain this state, we introduce an IR hardwall in the background AdS geometry. This results in a discrete spectrum of fermions. Next, we add a dynamical order parameter field and couple it to the fermions with (a relativistic extension of) a BCS type interaction. We solve then (in fixed background) the scalar-gauge-fermion system self-consistently and study the behavior of the order parameter as a function of the relative scaling dimension of the scalar and fermion fields. When translating the bulk physics to the boundary we find novel results namely that the order parameter have resonances for specific scaling dimensions. We speculate about the origin of these and point out that operator mixing in the boundary field theory has an important role when the bulk theory has interaction terms.

In Chapter 3 we study a Fermi surface coupled to a quantum critical boson in $d = 2$ dimensions defined in Section (1.1.4). As we have seen, this model has a relevant interaction between the boson order parameter and the fermion, therefore perturbation theory is not applicable. Because of the fermion sign problem, we cannot use numerical Monte-Carlo methods either. Unlike previous studies which mostly use renormalization group technique we investigate the problem with a different approach. We show that when one excludes fermion loops (which is called the quenched approximation in high-energy physics) it is possible to compute the fermion spectral function exactly using the linear nature of the fermion dispersion relation near the Fermi surface. As we expect the resulting state is not a Fermi liquid. Instead, the original Fermi surface splits and forms three singularities at low energies where the Green's function has power law behavior with different exponents.

In Chapter 4 we continue our investigation of this Hertz-Millis quantum critical metal by weakening our approximations and allow fermion loops to be present. We show that if the Fermi surface curvature is small,

in first approximation it is consistent to correct the boson two-point function only at one-loop order. With this modified propagator we carry out a similar computation than in Chapter 3 to obtain the fermionic Green's function. In the UV/intermediate energy range the quenched approximation is still valid but at lower energies different behavior was found. Deep in the IR the result is very similar to the RPA form using a strongly Landau damped boson. Therefore this calculation shows how to connect the quenched result with the Landau damping dominated low energy regime.

Bibliography

- [1] K. G. Wilson, "The renormalization group: critical phenomena and the Kondo," *Rev. Mod. Phys.* **47**, 4, 773.
- [2] E. Y. Loh, Jr., J. E. Gubernatis, R. T. Scalettar, S. R. White, D. J. Scalapino, and R. L. Sugar, "Sign problem in the numerical simulation of many-electron systems," *Phys. Rev. B* **41**, 9301 (1990).
- [3] M. Troyer and U.-J. Wiese, "Computational Complexity and Fundamental Limitations to Fermionic Quantum Monte Carlo Simulations," *Phys. Rev. Lett.* **94**, 170201 (2005), [cond-mat/0408370].
- [4] S. Durr *et al.*, "Ab-Initio Determination of Light Hadron Masses," *Science* **322**, 1224 (2008) [arXiv:0906.3599 [hep-lat]].
- [5] J. M. Maldacena, "The Large N limit of superconformal field theories and supergravity", *Adv. Theor. Math. Phys.* **2**, 231 (1998) [hep-th/9711200].
- [6] S. S. Gubser, I. R. Klebanov and A. M. Polyakov, "Gauge theory correlators from noncritical string theory", *Phys. Lett. B* **428** (1998) 105 [hep-th/9802109].
- [7] E. Witten, "Anti-de Sitter space and holography", *Adv. Theor. Math. Phys.* **2** (1998) 253 [hep-th/9802150].
- [8] Y. Liu, K. Schalm, Y.-W. Sun, J. Zaanen, "Holographic duality for condensed matter physics", Cambridge University Press, 2015
- [9] H. Liu, J. McGreevy and D. Vegh, "Non-Fermi liquids from holography", *Phys. Rev. D* **83** (2011) 065029 [arXiv:0903.2477 [hep-th]].
- [10] M. Cubrovic, J. Zaanen and K. Schalm, "String Theory, Quantum Phase Transitions and the Emergent Fermi-Liquid", *Science* **325** (2009) 439 [arXiv:0904.1993 [hep-th]].
- [11] S. W. Hawking, "Particle Creation by Black Holes", *Commun. Math. Phys.* **43** (1975) 199 [Erratum-ibid. **46** (1976) 206].

- [12] G. 't Hooft, “A Planar Diagram Theory for Strong Interactions,” Nucl. Phys. B **72** (1974) 461.
- [13] S. Sachdev, “Quantum phase transitions,” 2nd Edition, Cambridge University Press 2011
- [14] A. Bagrov, B. Mesznera and K. Schalm, “Pairing induced superconductivity in holography,” JHEP **1409**,106(2014) [arXiv:1403.3699 [hep-th]].
- [15] B. Mesznera, P. Säterskog, A. Bagrov and K. Schalm, “Non-perturbative emergence of non-Fermi liquid behaviour in $d = 2$ quantum critical metals,” Phys. Rev. B **94**, 115134, [arXiv:1602.05360 [cond-mat.str-el]].
- [16] B. Mesznera, P. Säterskog, and K. Schalm, “Non-perturbative correlation functions of a $d = 2$ quantum critical metal”, to be appear
- [17] J. A. Hertz, “Quantum critical phenomena,” Phys. Rev. B **14** (1976) 1165
- [18] M. A. Metlitski and S. Sachdev, “Quantum phase transitions of metals in two spatial dimensions: I. Ising-nematic order,” Phys. Rev. B **82** (2010) 075127 [arXiv:1001.1153 [cond-mat.str-el]]
- [19] M. A. Metlitski and S. Sachdev, “Quantum phase transitions of metals in two spatial dimensions: II. Spin density wave order,” Phys. Rev. B **82** (2010) 075128 [arXiv:1005.1288 [cond-mat.str-el]]
- [20] S. S. Lee, “Low-energy effective theory of Fermi surface coupled with U(1) gauge field in 2+1 dimensions,” Phys. Rev. B **80** (2009) 165102; [arXiv:0905.4532 [cond-mat.str-el]]
- [21] A. L. Fitzpatrick, S. Kachru, J. Kaplan and S. Raghu, “Non-Fermi liquid fixed point in a Wilsonian theory of quantum critical metals,” Phys. Rev. B **88** (2013) 125116 [arXiv:1307.0004 [cond-mat.str-el]]
- [22] A. L. Fitzpatrick, S. Kachru, J. Kaplan and S. Raghu, “Non-Fermi-liquid behavior of large- N_B quantum critical metals,” Phys. Rev. B **89** (2014) 16, 165114 [arXiv:1312.3321 [cond-mat.str-el]]

- [23] R. Mahajan, D. M. Ramirez, S. Kachru and S. Raghu, “Quantum critical metals in $d = 3 + 1$ dimensions,” Phys. Rev. B **88** (2013) 11, 115116 [arXiv:1303.1587 [cond-mat.str-el]]
- [24] G. Torroba and H. Wang, “Quantum critical metals in $4 - \epsilon$ dimensions,” Phys. Rev. B **90** (2014) 16, 165144 [arXiv:1406.3029 [cond-mat.str-el]]
- [25] A. V. Chubukov, and D. L. Maslov, “First-Matsubara-frequency rule in a Fermi liquid. I.: Fermion self-energy,” Phys. Rev. B **86** (2012) 15, 155136 [arXiv:1208.3483 [cond-mat.str-el]]
- [26] C. M. Varma, P. B. Littlewood, S. Schmitt-Rink, E. Abrahams and A. E. Ruckenstein, “Phenomenology of the normal state of Cu-O high-temperature superconductors,” Phys. Rev. Lett. **63**, 1996 (1989).
- [27] C. M. Varma, Z. Nussinov. W. van Saarloos, “Singular or non-Fermi liquids,” Physics. Reports **86** (2002) 5-6, [arXiv:1208.3483 [cond-mat.str-el]]
- [28] K. Andres, J. E. Graebner and H. R. Ott, “ $4f$ -Virtual-Bound-State Formation in CeAl₃ at Low Temperatures”, Phys. Rev. Lett. **35** (1975) 1779
- [29] A. W. Tyler and A. P. MacKenzie, “Hall effect of single layer, tetragonal $Tl_2Ba_2CuO_{6+\delta}$ near optimal doping”, Physica C 282-287 (1997) 1185-1186
- [30] R. Daou *et al.*, “Broken rotational symmetry in the pseudogap phase of high- T_c superconductor,” Nature **463**, 519-522 (2009), [arXiv:0909.4430 [hep-lat]].
- [31] C. Varma, “High-temperature superconductivity: Mind the pseudogap,” Nature **468**, 184-185 (2010)
- [32] T. Faulkner, H. Liu, J. McGreevy and D. Vegh, “Emergent quantum criticality, Fermi surfaces, and AdS(2),” Phys. Rev. D **83**, 125002 (2011) [arXiv:0907.2694 [hep-th]].
- [33] N. Iqbal, H. Liu and M. Mezei, “Semi-local quantum liquids,” JHEP **1204**, 086 (2012) [arXiv:1105.4621 [hep-th]].

- [34] S. S. Lee, “A Non-Fermi Liquid from a Charged Black Hole: A Critical Fermi Ball,” *Phys. Rev. D* **79**, 086006 (2009) [arXiv:0809.3402 [hep-th]].
- [35] S. S. Gubser and F. D. Rocha, “Peculiar properties of a charged dilatonic black hole in AdS_5 ,” *Phys. Rev. D* **81**, 046001 (2010) [arXiv:0911.2898 [hep-th]].
- [36] K. Goldstein, S. Kachru, S. Prakash and S. P. Trivedi, “Holography of Charged Dilaton Black Holes,” *JHEP* **1008**, 078 (2010) [arXiv:0911.3586 [hep-th]].
- [37] C. Charmousis, B. Gouteraux, B. S. Kim, E. Kiritsis and R. Meyer, “Effective Holographic Theories for low-temperature condensed matter systems,” *JHEP* **1011**, 151 (2010) doi:10.1007/JHEP11(2010)151 [arXiv:1005.4690 [hep-th]].
- [38] B. Gouteraux and E. Kiritsis, “Generalized Holographic Quantum Criticality at Finite Density,” *JHEP* **1112**, 036 (2011) [arXiv:1107.2116 [hep-th]].
- [39] Z. Bajnok and R. A. Janik, “Four-loop perturbative Konishi from strings and finite size effects for multiparticle states,” *Nucl. Phys. B* **807**, 625 (2009) [arXiv:0807.0399 [hep-th]].
- [40] N. Arkani-Hamed, F. Cachazo and J. Kaplan, “What is the Simplest Quantum Field Theory?,” *JHEP* **1009**, 016 (2010) [arXiv:0808.1446 [hep-th]].
- [41] D. Chowdhury, S. Raju, S. Sachdev, A. Singh and P. Strack, “Multipoint correlators of conformal field theories: implications for quantum critical transport,” *Phys. Rev. B* **87**, no. 8, 085138 (2013) [arXiv:1210.5247 [cond-mat.str-el]].
- [42] K. Skenderis, “Lecture notes on holographic renormalization,” *Class. Quant. Grav.* **19**, 5849 (2002) [hep-th/0209067].
- [43] J. Zaanen, “A Modern, but way too short history of the theory of superconductivity at a high temperature,” [arXiv:1012.5461 [cond-mat.supr-con]].

- [44] G. Bednorz and K. A. Müller, “Possible high- T_c superconductivity in the $Ba - La - Cu - O$ system,” *Physik B - Condensed Matter* (1986) 64: 189.
- [45] A. V. Ramallo, “Introduction to the AdS/CFT correspondence,” *Springer Proc. Phys.* **161**, 411 (2015) [arXiv:1310.4319 [hep-th]].
- [46] H. Bruus and K. Flensberg, “Many-Body Quantum Theory in Condensed Matter Physics,” Oxford University Press 2004
- [47] S. A. Hartnoll and A. Tavanfar, “Electron stars for holographic metallic criticality,” *Phys. Rev. D* **83**, 046003 (2011) [arXiv:1008.2828 [hep-th]].
- [48] T. Faulkner and J. Polchinski, “Semi-Holographic Fermi Liquids,” *JHEP* **1106**, 012 (2011) [arXiv:1001.5049 [hep-th]].
- [49] J. Kaplan, “‘Lectures on AdS/CFT from the Bottom Up’”, <http://sites.krieger.jhu.edu/jared-kaplan/files/2016/05/AdSCFTCourseNotesCurrentPublic.pdf>

